



**UNIVERSITI
TEKNOLOGI
PETRONAS**

Numerical Investigation of “On Roof Solar-Biomass Chimney”

by

Noorul Haskin Binti Mukthar Rahman

M6979

**Dissertation submitted in partial fulfillment of
the requirements for the
Bachelor of Engineering (Hons)
(Mechanical Engineering)**

JANUARY 2009

Universiti Teknologi PETRONAS

Bandar Seri Iskandar

31750 Tronoh

Perak Darul Ridzuan

CERTIFICATION OF APPROVAL

Numerical Investigation of “On Roof Solar-Biomass Chimney”

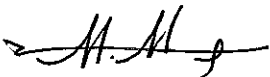
by

Noorul Haskin Binti Mukthar Rahman

M6979

**A project dissertation submitted to the
Mechanical Engineering Programme
Universiti Teknologi PETRONAS
in partial fulfilment of the requirement for the
BACHELOR OF ENGINEERING (Hons)
(MECHANICAL ENGINEERING)**

Approved by,



(AP Dr. Hussain Al-Kayiem)

**UNIVERSITI TEKNOLOGI PETRONAS
TRONOH, PERAK**

January 2009

CERTIFICATION OF ORIGINALITY

This is to certify that I am responsible for the work submitted in this project, that the original work is my own except as specified in the references and acknowledgements, and that the original work contained herein have not been undertaken or done by unspecified sources or persons.



NOORUL HASKIN BT MUKTHAR RAHMAN

ACKNOWLEDGEMENTS

Alhamdulillah, first and foremost, I thanked ALLAH the Almighty for His blessings and guidance throughout this final year. Not forgetting my family especially my parents and brothers, sincere gratitude for their love and continuous support.

I also would like to thank UTP for providing me a place to further my studies and complete my Final Year Project (FYP).

My greatest gratitude to my FYP Supervisor, AP Dr Hussain Al-Kayiem, for his guidance, support and understanding which make me feel comfortable and enjoy doing the FYP. Thanks for his opinion, comments, ideas, and encouragement that he give to me to finish this project. This project would not be success without his supervision and advice. I am very lucky to have him as my supervisor.

Warmest gratitude to my colleagues particularly FYP students who are also doing CFD simulations since they share their information and help me to solve the problem with FLUENT and GAMBIT. This special thanks and appreciation are dedicated to:

- ★ Mohd Firdaus Sidik
- ★ Mohammed Fathelrahman
- ★ Ahmad Safuan
- ★ Ricky Tan Kien Weng
- ★ Khor Yin Yin
- ★ Nur Liyana Farizah
- ★ Final Year Mechanical students

Finally, thanks to all people that directly or indirectly contribute to the successful of this final year project.

ABSTRACT

Sun intensity is different according to its angle of radiation. North and south or east or west of a building will receive different solar intensity. The radiation also affected by the inclination of the surface where sun radiates. Thus, the effect of the different configurations is investigated. The radiation intensity for the collector and canopy in the on-roof solar chimney is different since the material used is different which resulted in different temperature. This difference in temperature will be a significant effect in analyzing the output of the solar chimney. The methods and analysis are done using Computational Fluid Dynamics (CFD) software such as GAMBIT and FLUENT. The analysis was also done for three cases with different configurations. Case 1 consists of Configuration 1 (trimmed-inlet) and Configuration 2 (flat-inlet). The configurations were analysed with two options of temperature distribution, Option A (same temperature for left and right side of roof) and Option B (different temperature for left and right side of roof). Case 2 have two different heat transfer consideration for the collector either conduction or convection and is analysed for three different inlet diameter. Case 3 is solar-biomass integration chimney configurations. From the simulation particularly from FLUENT, the outlet velocity is different for different geometry configurations and operating conditions.

TABLE OF CONTENT

CERTIFICATION OF APPROVAL	i
CERTIFICATION OF ORIGINALITY.....	ii
ACKNOWLEDGEMENTS.....	i
ABSTRACT	i
TABLE OF CONTENT	i
LIST OF FIGURE	iv
LIST OF TABLES	vi
CHAPTER 1 INTRODUCTION	1
1.1 Background	2
1.2 Problem Statement	2
1.3 Objectives:.....	3
1.4 Scope of Study	3
1.5 Significance of Work	3
CHAPTER 2 LITERATURE REVIEW	4
CHAPTER 3 THEORY	14
3.1 Heat and fluid flow.....	14
3.2 Heat transfer on collector	15
3.3 Heat transfer to air.....	16
3.4 Heat transfer inside channel	18
3.5 Turbulent Viscous Model.....	19

3.5.1	The RNG k- ϵ Model	19
3.5.2	Transport Equations for the RNG k- ϵ Model	20
3.5.3	Modeling the Effective Viscosity	21
3.5.4	RNG Swirl Modification	22
3.5.5	Calculating the Inverse Effective Prandtl Numbers	23
3.6	Area and Diameter Calculation for FLUENT input.....	23
CHAPTER 4 METHODOLOGY		24
4.1	Tools.....	24
4.2	Technique of Analysis.....	24
4.3	Procedures	25
4.4	Work Flow Execution	30
4.5	Gantt Chart.....	31
CHAPTER 5 RESULT & DISCUSSION		33
5.1	Sample of Fluent Result.....	33
5.1.1	Different Inlet Configuration Results.....	33
5.1.2	Different Case Results.....	36
5.2	Temperature and Velocity Plot	39
5.2.1	Case 1, Configuration 1, Option A.....	39
5.2.2	Case 1, Configuration 1, Option B	40
5.2.3	Case 1, Configuration 2, Option A.....	41
5.2.4	Case 1, Configuration 2, Option B	42
5.2.5	Case 2, Configuration 3, Option 1a.....	43
5.2.6	Case 2, Configuration 3, Option 1b.....	44
5.2.7	Case 2, Configuration 3, Option 1c.....	45

5.2.8 Case 2, Configuration 3, Option 2a.....46

5.2.9 Case 2, Configuration 3, Option 2b.....47

5.2.10 Case 2, Configuration 3, Option 2c.....48

5.2.11 Case 2, Configuration 4, Option 1a.....49

5.2.12 Case 2, Configuration 4, Option 1b.....50

5.2.13 Case 2, Configuration 4, Option 1c.....51

5.2.14 Case 2, Configuration 4, Option 2a.....52

5.2.15 Case 2, Configuration 4, Option 2b.....53

5.2.16 Case 2, Configuration 4, Option 2c.....54

5.2.17 Case 3, Configuration 5.....55

5.2.18 Case 3, Configuration 6.....56

5.3 Velocity, Temperature and Mass Flow Rate..... 57

5.4 Discussion 58

CHAPTER 6 CONCLUSION & RECOMMENDATIONS.....59

6.1 Conclusion 59

6.2 Recommendations 59

REFERENCES.....61

APPENDIX..... 63

LIST OF FIGURE

Figure 1.1 - Estimated percentage contributions to world renewable energy supplies, 2001. Total: 83 EJ (main sources: IEA, 2003; BP, 2003). Solar includes both solar thermal and solar photovoltaic energy	1
Figure 2.1 - Solar Chimney plus Bell Jar (SCBJ)	6
Figure 2.2 - Solar Chimney configurations.....	7
Figure 2.3 - Operation of Solar Chimney	8
Figure 2.4 - The overall heat network.....	9
Figure 2.5 - Conceptual operation of a solar roof collector	10
Figure 2.6 -Principle of the solar chimney: glass roof collector, chimney tube, wind turbines.....	11
Figure 2.7 - Modeling of the thermo fluid mechanism in half side of the roof	12
Figure 2.8 - Heat transfer networking in the Roof Solar Chimney system.....	12
Figure 2.9 - Experimental apparatus	13
Figure 3.1- Cross sectional layer of Cover and Collector.....	15
Figure 3.2 - Parameter used in the numerical simulations	16
Figure 3.3-Flow velocity difference between laminar and turbulent flows	18
Figure 4.1-Dimension of the roof and chimney drawing for case 1	26
Figure 4.2-GAMBIT drawing for case 2	27
Figure 4.3-Dimension of the roof and chimney drawing for case 3	28
Figure 4.4-Work Flow Chart.....	30

Figure 5.1- Case11A-From top to bottom; left to right: 33

Figure 5.2- Case12A-From top to bottom; left to right: 34

Figure 5.3-Case232-From top to bottom; left to right: 34

Figure 5.4-Case242-From top to bottom; left to right: 35

Figure 5.5 -Case 11A-From top to bottom; left to right: Temperature Contour, Velocity Contour, Temperature Contour Mesh, Velocity Contour Mesh, and Velocity Vector 36

Figure 5.6- Case 2311-From top to bottom; left to right: Temperature Contour, Velocity Contour, Temperature Contour Mesh, Velocity Contour Mesh, and Velocity Vector 37

Figure 5.7 - Case35- From top to bottom; left to right: Temperature Contour, Velocity Contour, Temperature Contour Mesh, Velocity Contour Mesh, and Velocity Vector 38

Figure 5.8 - Justification for higher velocity result..... 58

LIST OF TABLES

Table 4.1- Case 1 to be investigated	25
Table 4.2-Case 2 to be investigated	27
Table 4.3-Case 3 to be investigated	28
Table 4.4-Terms description for each configuration.....	28
Table 4.5 - Option A and Option B details	29
Table 4.6-Materials used in solar chimney system	29
Table 4.7 - Schedule for First Semester of Final Year Project (FYP I).....	31
Table 4.8 - Schedule for Second Semester of Final Year Project (FYP II)	32
Table 5.1 - FLUENT result on chimney outlet velocity and temperature with mass flow rate from outlet for different configurations and conditions.....	57
Table 5.2 - FLUENT result on different types of collector plate.....	58

ABBREVIATION & NOMENCLATURES

FYP	=	Final Year Project
CFD	=	Computational Fluid Dynamics
RNG	=	Re-Normalization Group
Nu	=	Nusselt number
Ra_L	=	Rayleigh number
Re	=	Reynolds number
Pr	=	Prandtl number
\bar{h}	=	Convection coefficient
ε	=	Emissivity
ρ	=	Density
V	=	Velocity
σ	=	Stefan-Boltzman constant
τ	=	Transmissivity
k	=	Thermal conductivity
ν	=	Kinematic viscosity
β	=	Volumetric thermal expansion coefficient
g	=	Gravitational acceleration

α	=	Absorptivity
T_{in}	=	Chimney inlet temperature
T_{out}	=	Chimney outlet temperature
ΔT	=	Temperature difference in chimney
T_s	=	Collector surface temperature
T_∞	=	Ambient temperature
T_m	=	Mean temperature
L_c	=	Characteristic length
A_s	=	Surface area
P	=	Perimeter
D_{in}	=	Inlet diameter
D_h	=	Hydraulic diameter
I	=	Solar intensity
θ	=	Inclination angle
\dot{m}	=	Mass flow rate

CHAPTER 1

INTRODUCTION

This chapter briefed on the introduction of the FYP project on Numerical Investigation of “On Roof Solar-Biomass Chimney”. The project is focused in optimizing the renewable energy. The principal source of renewable energy is solar radiation. Using solar collectors, the radiation can provide hot water or space heating. Solar radiation can be converted to useful energy indirectly, via other energy form such as bioenergy. Biomass is a type of waste which includes tree and shrubs, agricultural, all forms of human, animal and plant waste, etc that can be converted into energy. Biomass can be converted in useful forms of energy by combustion, dry chemical process and aqueous process.

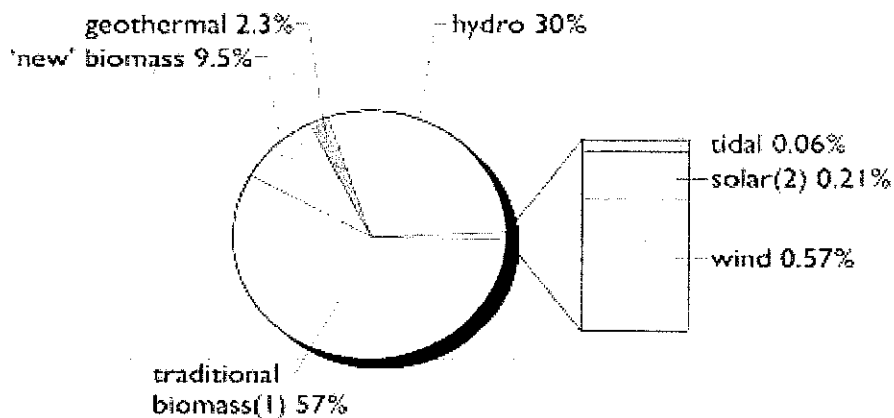


Figure 1.1 - Estimated percentage contributions to world renewable energy supplies, 2001. Total: 83 EJ (main sources: IEA, 2003; BP, 2003). Solar includes both solar thermal and solar photovoltaic energy

From figure1.1, there are many sources of renewable energy. Solar energy, as well as wind, resource is a promising clean resource compromising the following features:

- No political impact in the sustainability and in the pricing policy of the sources.
- Environmental friendly.
- Renewable and sustainable resources.

Biomass, in the form of wood or other 'biofuels', is a major world energy source, especially in the developing world which is also consider for the enhancement of this project.

1.1 Background

In recent times, there are new exploitations from solar source. Solar chimney is used for different applications in many countries. Usually, solar chimney or also known as thermal chimney is a way of improving the natural ventilation of buildings. An innovative power generation method was founded where electricity can be produced from the on roof solar chimney and the studies on improving the efficiency are carried out. On roof solar chimney may developed for electricity generation using Savonius wind turbine.

1.2 Problem Statement

The power generation was analyzed with the present of solar radiation from the sun. To continue the power generation for whole day, the use of biomass was developed to compensate the absence of sun during night and cloudy time. The analysis was limited to single geometry configuration and further configuration required to be investigated. A better computer aid is needed to observe the flow pattern of the fluid flow in solar chimney.

1.3 Objectives:

1. To model the on roof solar chimney system.
2. To simulate numerically the on Roof Solar-Biomass Chimney using CFD and analyze the flow and heat transfer in the system.
3. To investigate, numerically, the chimney performance at different operational conditions and different geometry configurations.

1.4 Scope of Study

The FYP project covers numerical investigation of the system and computational part using computational fluid dynamics (CFD) software. There are needs to simulate various configurations of roof and chimney using GAMBIT and FLUENT software to optimize the design parameter. The study of solar and biomass integration also will be performed.

1.5 Significance of Work

Numerical investigation need to be done to get a better results and to proceed with the implementation. The numerical analysis was intended to predict the flow pattern in the chimney and would help in design criteria. CFD simulations are able to demonstrate the optimization of the electricity generation. Thus, simulations from approved software are planned to be carried out by the student in order to help the research group to achieve their objectives. This research is also would be a solution for people in Sabah who are suffering of inadequate of electric supply.

CHAPTER 2

LITERATURE REVIEW

The On Roof Solar-Biomass Chimney is a small scale application of power generation which is planned for domestic use. To obtain the desired power generation, the air velocity must be high enough to rotate the Savonius rotor. Thus, optimum solar radiation and the ideal chimney position must be achieved. The analysis and the result are expected from the Computational Fluid Dynamics (CFD) simulation by using Gambit and Fluent software.

The On Roof Solar-Biomass Chimney is an enhanced application from solar chimney and roof solar chimney. Solar Chimney is widely used for building ventilation. The ventilation is categorized as natural ventilation where it can be categorized as wind driven ventilation and stack ventilation. According to Joseph (1999), nowadays, natural ventilation is not only used to provide fresh air for the occupants but also as an excellent energy-saving way to reduce the internal cooling load of housing located in the tropics.

From the experiment conducted by Joseph (1999), the air which is driven by buoyancy is continuously induced through the building with a rate depends mainly on intensity of incident solar radiation. 0.04m/s air motion cannot satisfy occupants and higher velocity of 2m/s is needed. The air motion could be increased by increasing the number of units of

solar chimneys on roof, eastern and western walls and by installing several free openings at the northern façade of the room.

A study was carried out by Joseph (2001) to examine the performance of solar chimney within an air-conditioning building. It is concluded that the solar chimney reduces the accumulation of the building heat continuously. The solar chimney house consumes 10-20% less electrical power compared with the common house.

Meanwhile papers from Jothirmay (2005) stated that at Jaipur (India), 45° of chimney inclination is found to be optimum for obtaining maximum rate of ventilation. It is 10% higher compared to 60° and 30° inclinations. To predict the performance solar chimney, study of heat transfer through natural convection was conducted. Parameters included are: temperature of air inlet and outlet, ambient temperature, flow velocity, area inlet and outlet opening. The assumptions made were steady state conditions and laminar air flow in channel. The Energy Balance was written as below;

For glass cover,

$$q_{\text{rad}} + q_{\text{rad,wall}} = q_{\text{conv}} + h_{\text{loss,glass}}$$

[incident solar radiation]+[radiative heat gain by glass cover from absorber wall]=
[convective heat loss to air in flow channel]+[overall heat loss coefficient from glass to ambient]

For air

$$q_{\text{conv,abs}} + q_{\text{conv,glass}} = h_{\text{gain}}$$

[convection from absorber]+[convection from glass]=[useful heat gain by the air]

For absorber

$$I = q_{\text{conv}} + q_{\text{rad(long wave)}} + q_{\text{cond}}$$

[solar radiation]=[convection to air in flow channel]+[long wave re-radiation to glass]+
conduction to main room]

It also established that the flow increases as the inlet height increases.

A thought experiment was suggested by Alan (2005) from the idea of solar chimney in Manzanares, Spain using Convective Energy Conversion Cycle (CECC). The system is known as Solar Chimney plus Bell Jar.

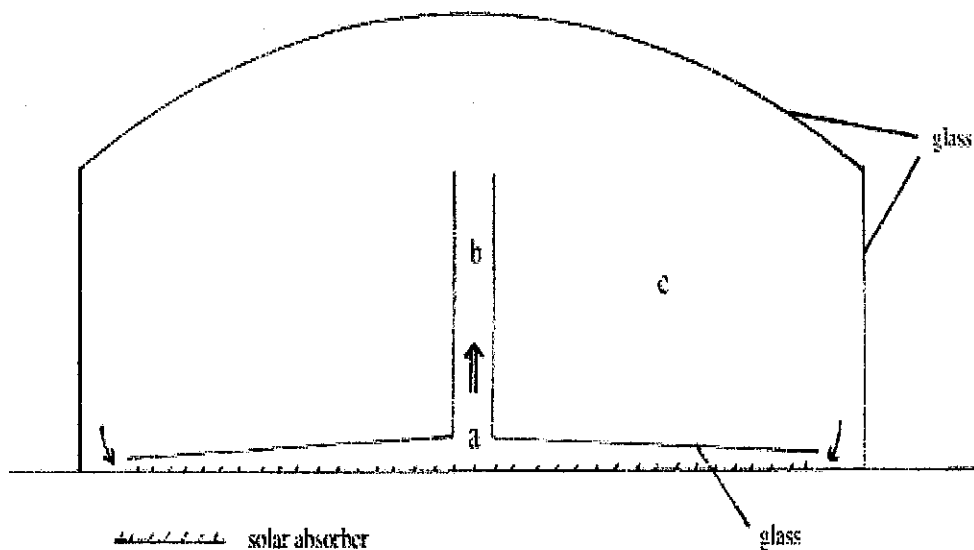


Figure 2.1 - Solar Chimney plus Bell Jar (SCBJ)

The solar absorber remains the driver of the system. In this closed configuration, as solar energy is taken up by the absorber, the total volume of air inside the bell jar cannot expand. A flow pattern will be established taking air from (a) to (b) to (c) and return to (a). This will transport energy from the absorber to the turbines which export energy and through the large expanse of the bell jar where some energy will be lost through the glass.

Alan concluded that the only loss of energy is through the glass of the bell jar and the result is solar energy will be converted into electricity with very high efficiency.

Design of solar chimney especially on roof solar chimney, must take into account the architectural integrity of building while giving importance in providing efficient air movement. Factors influencing the chimney design are the location, climate, building orientation, size of building to be ventilated and internal heat gains (Harris, 2006).

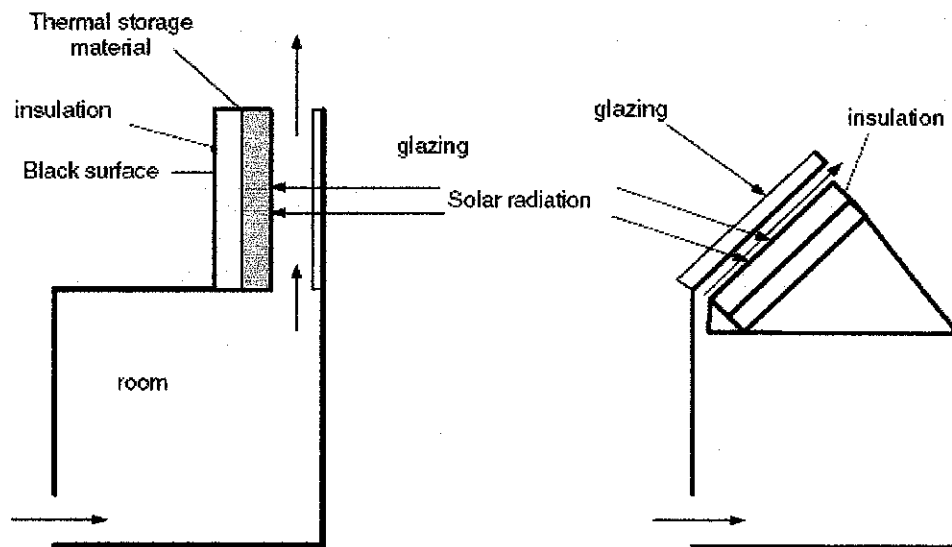


Figure 2.2 - Solar Chimney configurations

As explained by Harris (2006), the basic principle of a solar chimney is illustrated in figure below. Solar radiation passes through glazing and absorbed at the wall surface. The air in the chimney then heated by convection and radiation from the absorber. The heated air becomes hot and less dense thus moving upward through the chimney. The cool air from the building or the room will replace the air in the chimney and create continues process.

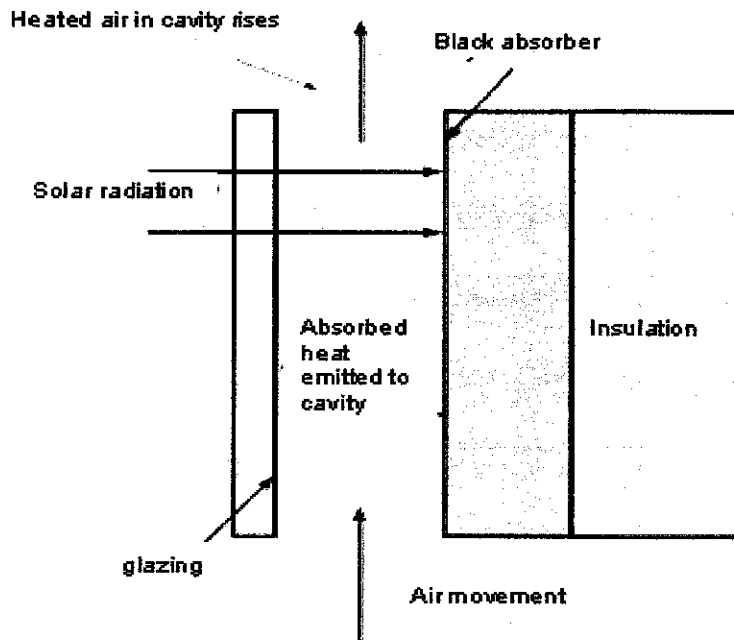


Figure 2.3 - Operation of Solar Chimney

A paper produced by A.Murthi (2006), carried out CFD simulation to evaluate the solar induced ventilation in terrace house model in Malaysia. Base on the simulation result, the average air velocity in the pipe is 0.1m/s. His paper concluded from his research and previous research that air velocity without considering the wind effect is influenced by climate parameters (solar radiation and ambient temperature). The low indoor air velocity and high ambient temperature may create unwanted negative ventilation by limiting room design parameters in terrace house. Optimum design parameters (height, width, length and material) of a vertical solar chimney can be deduced by comparing simulation results based on previous research.

Research done by Harris (2006) was assisted by CFD model with heat network. Heat network is solved in a conventional way using basic equations and heat transfer

correlations. The governing process is the basic stack effect where it states that warmer air experiences an upward pressure in relation to cooler air, due to decrease in density.

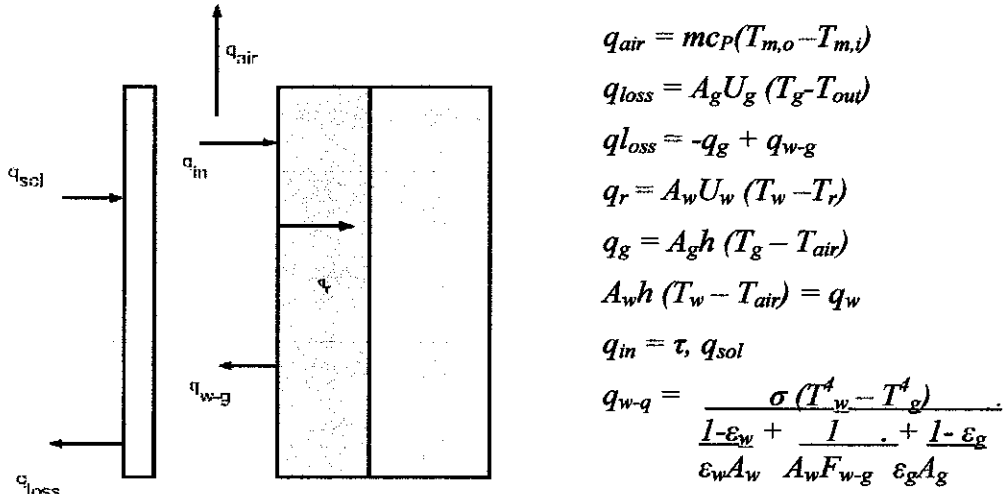


Figure 2.4 - The overall heat network

After prediction of the surface and air-conditions and mean flow, the results were entered into CFD program to evaluate actual flow characteristics. Heat transfer coefficients were calculated using Nusselt Number, conductivity of air and hydraulic meter.

$$h = Nu k / D_h$$

$$\text{where } Nu = f(Re_D, Pr)$$

From the experiment, it is concluded that maximum air flow is given with the low emissivity and cavity width of 0.25m and minimum flow is given by double glazing high emissivity and cavity of 0.1m. Varying the slope of the chimney resulted in variations in the performance where the flow rate increases for up to 67.5° (angle of inclination), and for lower angles than 45° the flow reduces.

A successful simulation was done using FLUENT software by Tan (2007) on flow driven by natural convection in a solar roof collector operating at peak midday conditions in Malaysia.

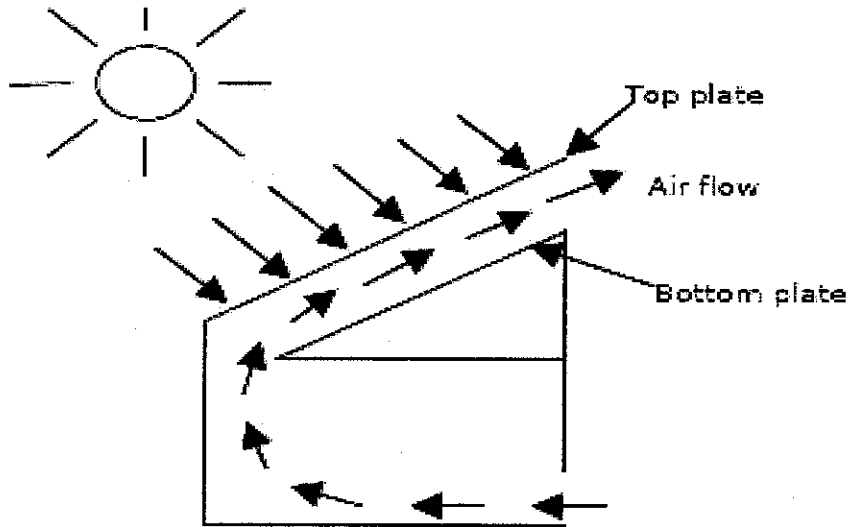


Figure 2.5 - Conceptual operation of a solar roof collector

The flow is assumed to be two-dimensional, steady state and laminar based on the low air speeds in the air gap and the living space shields the inlet stream from atmospheric disturbances. The momentum, continuity and energy equation are solved using the coupled solver. The computational domain is placed horizontally and by varying the gravity direction, various inclinations are modeled.

Ali Nazarian (2007) have highlighted that the heat transfer of air by convection is a combination of natural convection and forced convection. Thus Nu used in calculation for the on roof solar chimney is

$$Nu^n = Nu_F^n + Nu_N^n$$

Where

$n=3$ is suggested for laminar and turbulent starts

Nu_N = natural convection correlations

Nu_F = forced convection correlations

The solar chimney has been initiated by America, Spain, China, India, Australia and Turkey in the effort to find a cleaner and abundant source of energy. These projects have been in the form of large solar power plants that could generate MWatts of power. The first planning of a pilot power plant has been carried out and its construction started at Manzanares-Spain, Haff, et al, 1981. Then after, the solar chimney has been subjected to numerous experimental, theoretical and numerical analyses (Hussain, 2008).

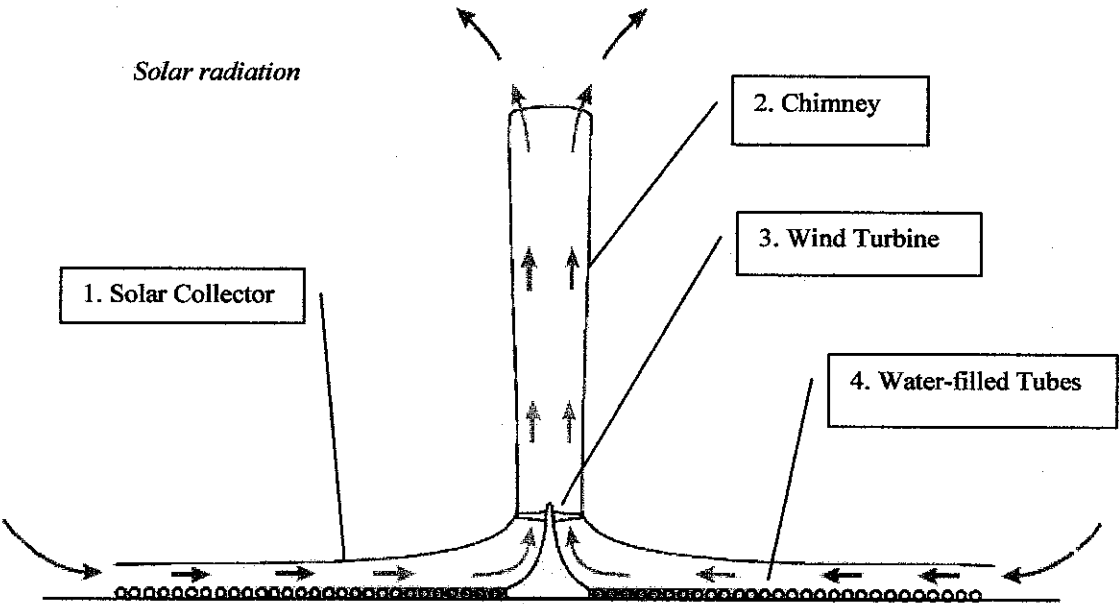


Figure 2.6 -Principle of the solar chimney: glass roof collector, chimney tube, wind turbines

Robert (2008) had come out with an analysis of the on roof solar chimney in conjunction with the optimization of flue gases heat to run the rotor inside the chimney. Figure below shows his analytical drawing of thermo fluid mechanism modeling on roof solar chimney.

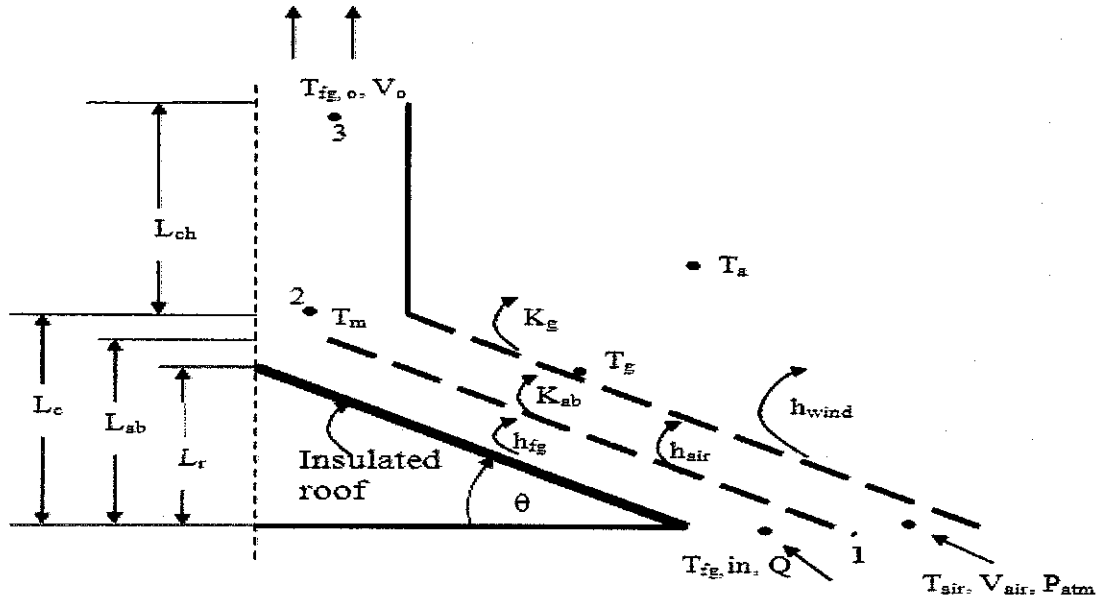


Figure 2.7 - Modeling of the thermo fluid mechanism in half side of the roof

The system consists of three layers of materials producing two passages. The outer layer is the canopy which is made of transparency material. The intermediate layer is made of corrugated metal sheet black painted in the upper surface to absorb as high as possible of solar radiation. The third layer is insulator covers the original roof to prevent the heat to transfer to the interior of the house.

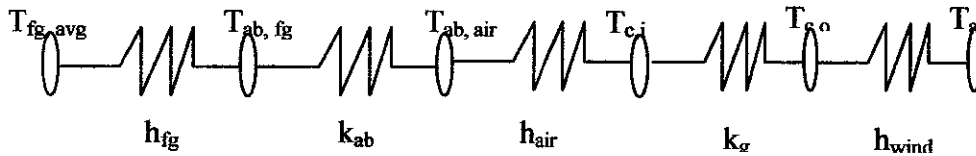


Figure 2.8 - Heat transfer networking in the Roof Solar Chimney system

A suggestion to maintain the efficiency of the roof chimney is given by Norhusna (2008) where by increasing the thickness of the collector; more heat could be absorbed and stored in collector. Later these heats slowly dissipate during night and still manage to create airflow although the efficiency is lower than the daytime.

CFD modelling was done by A.Murthi and M.Hamdan for Solar Induced Ventilation. From the result, air velocity on the trombe wall and solar chimney model can increase air flow up to 0.5m/s while solar roof until 0.3m/s. This depends on the opening position and the experiment was run where the air velocity zone for solar chimney model was broader than trombe wall.

Zoltan has done detailed mathematical simulation and experimental investigation of airflow in solar chimneys. The chimney is divided into a large number of blocks from the bottom to the top; a multi-zone model can be constructed. The model takes the buoyancy effect, friction losses, radiation, convective and conductive heat transfers into account. The experimental apparatus is a chimney channel with changeable channel thickness and inclination angle. Electrically heated panels below the aluminum wall surface provided the heat flux. The backside was heavily insulated. The conclusion was the simulation model is able to predict flow rates for a wide range of variables although there are some differences.

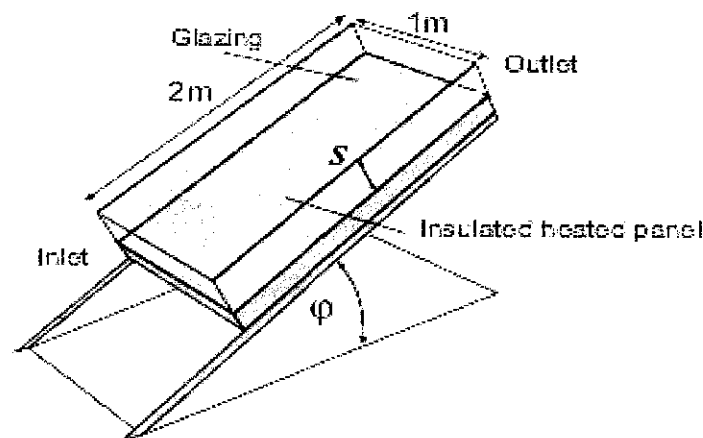


Figure 2.9 - Experimental apparatus

CHAPTER 3

THEORY

In this theory part, the basic equation of heat transfer and energy balance equation are explained. The governing equations were obtained during the study of literature survey. Since the on roof solar chimney is exposed to atmosphere and solar radiation, there are several types of heat transfer through the parts of the on roof solar chimney. Parts that are taken into consideration are such as canopy (transparent cover) and collector (absorber) which experienced heat transfer of convection and radiation on. The temperature, heat and fluid flow of the air are also important in evaluating the performance of the solar chimney.

3.1 Heat and fluid flow

The top part of the on roof solar chimney, which is canopy is heated by solar radiation. The radiation passes through the transparent cover (canopy) where some radiation is reflected, $q_{\text{rad,cover}}$ and some are absorbed, $q_{\text{abs,cover}}$. However, those amounts are negligible. A portion of the solar radiation will be absorbed by the collector which is painted black. On the collector, there are two types of energy which are energy reflected from the collector, $q_{\text{rad,collector}}$ and the energy absorbed by the collector, $q_{\text{abs,collector}}$. The collector would heat up the surrounding air by natural convection which results in temperature increase of the air and the density decrease due to expansion. Thus the air gain energy, $q_{\text{conv,air}}$ and provide the driving force for the Savonius rotor.

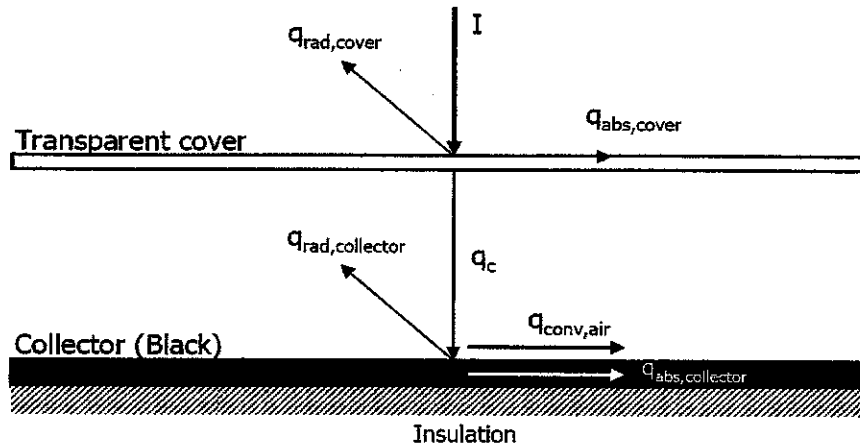


Figure 3.1- Cross sectional layer of Cover and Collector

3.2 Heat transfer on collector

The total energy input gained by collector can be described using equation below;

$$q_c = \tau_{\text{glass}} \times I \times \alpha_c \times A_c$$

Where

τ_{glass} = Transmissivity of the cover

I = Solar intensity

α_c = Absorptivity of the collector

A_c = Area of the collector

Transmissivity is fraction of the incident radiation passing through the cover while absorptivity is fraction of the incident radiation absorbed by the collector. Usually glass has higher transmissivity and collector which painted in black also provides higher radiation absorption. This criterion help in enhancing the heat transfer of the collector. Solar intensity in Malaysia by average is known to be 700-800W/m². To maximize the effective heat transfer process, larger area is designed using corrugated shape collector. To reduce the losses of heat absorbed into the house or the building, insulation is applied below the collector.

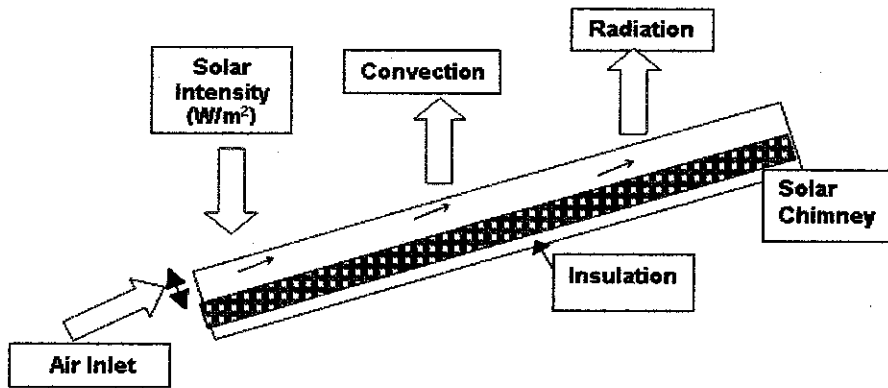


Figure 3.2 - Parameter used in the numerical simulations

The output energy is the summation of energy loss due to radiation $q_{\text{rad, collector}}$ and the transfer of energy absorbed by the collector to adjacent air (which is equal to energy gained by the air), $q_{\text{conv, air}}$.

$$q_{\text{rad collector}} = \epsilon \sigma (T_s^4 - T_a^4) A_c$$

Where

ϵ = Emissivity of the collector

σ = Stefan-Boltzman constant

T_s = Surface temperature of collector

T_a = Air temperature at inlet

A_c = Area of the collector

3.3 Heat transfer to air

Heat gained by the collector is transferred to surrounding by **convection** which is due to temperature difference between surface and air.

$$q_{\text{conv, air}} = A_c \times \bar{h} \times (T_s - T_m)$$

Where

A_c = Area of the collector

\bar{h} = Mean convection heat transfer coefficient

$$= \bar{h} = \frac{k \times \overline{Nu}}{L_c}$$

(Where

k = thermal conductivity of air at T_m , Nu = Nusselt number, L_c = characteristic length)

T_s = Surface temperature of collector

T_m = Mean temperature of the air

$$= (T_s + T_a)/2$$

(where T_a = Air temperature at inlet)

Nu accounts for both convection and conduction heat transfer.

$$Nu = \frac{hL}{k} \rightarrow \frac{hL}{k} \cdot \frac{\Delta T}{\Delta T} = \frac{h\Delta T}{k \frac{\Delta T}{L}} \begin{matrix} \longrightarrow & \text{Convection heat transfer} \\ \longrightarrow & \text{Conduction heat transfer} \end{matrix}$$

The convection process is expected to be a combination of natural and force convection. Thus, the resultant Nusselt Number, Nu is combination of forced convection correlations, Nu_F and natural convection correlations, Nu_N ;

$$Nu^n = Nu_F^n + Nu_N^n$$

where $n=3$ is suggested for laminar and turbulent starts

Nu is also incorporates a number of correlations for various conditions with respect to Reynolds, Re and Prandtl number, Pr .

$$Nu = f(Re, Pr)$$

$$\text{Thus, } h_{\text{air}} = k_{\text{air}} \times Nu_{D,\text{air}} / D$$

3.4 Heat transfer inside channel

$$\text{Prandtl, } Pr = \frac{\nu}{\alpha}$$

where

ν = flow property relative to the momentum

α = thermal property relative to diffusivity

Nature of motion of particles makes it laminar or turbulent.

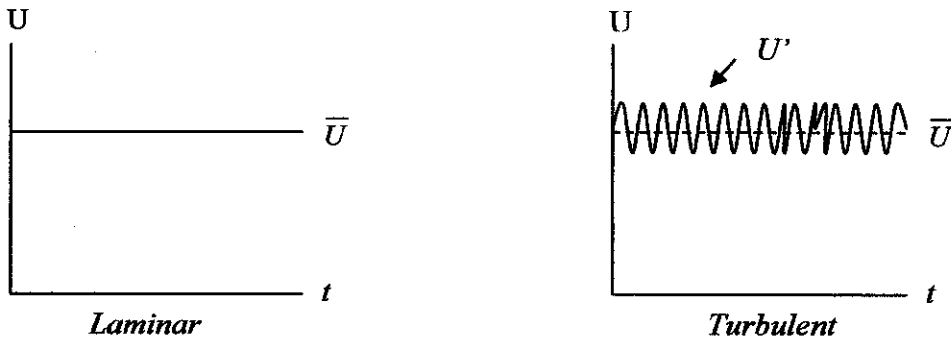


Figure 3.3-Flow velocity difference between laminar and turbulent flows

Thus, for turbulence, the flow is $U = \bar{U} \pm U'$ where U' is the turbulent part in the flow. To compensate the fluctuation of the flow, k- ϵ model is used.

From the free convection empirical correlations for inclined plates (cold surface up or hot surface down), the recommended correlation is

$$\overline{Nu}_L = \left\{ 0.825 + \frac{0.387 Ra_L^{1/6}}{\left[1 + (0.492 / Pr)^{9/16} \right]^{8/27}} \right\}^2, \quad g \rightarrow g \cos \theta$$

And the restrictions is $0 \leq \theta \leq 60^\circ$

$$Ra_L = \frac{g\beta(T_s - T_\infty)L^3}{\nu\alpha}$$

where

$$\beta = \frac{1}{T_m}, \quad T_m = \frac{(T_s + T_\infty)}{2}$$

3.5 Turbulent Viscous Model

The flow is assumed to be turbulent flow with K-ε (epsilon) model, specifically, Re-Normalisation Group (RNG) model. RNG is better than Standard model because this model renormalise the Navier-Stokes equations and to account for the effects of smaller scales of motion.

The flow of air in the chimney is low turbulent. Thus, k-ε model is preferable. Since the flow has low Reynolds number (Re), RNG k-ε model is suitable than Standard k-ε model. It is because Standard k-ε model is used for high turbulence model and is not suitable for low turbulence model. Using this model, the turbulence specification method is chosen to be intensity and hydraulic diameter instead of K and Epsilon to get better result.

3.5.1 The RNG k-ε Model

The RNG k-ε model was derived using a rigorous statistical technique (called renormalization group theory). It is similar in form to the standard k-ε model, but includes the following refinements:

- The RNG model has an additional term in its ε equation that significantly improves the accuracy for rapidly strained flows.
- The effect of swirl on turbulence is included in the RNG model, enhancing accuracy for swirling flows.
- The RNG theory provides an analytical formula for turbulent Prandtl numbers, while the standard k- ε model uses user-specified, constant values.
- While the standard k- ε model is a high-Reynolds-number model, the RNG theory provides an analytically-derived differential formula for effective viscosity that accounts for low-Reynolds-number effects. Effective use of this feature does, however, depend on an appropriate treatment of the near-wall region.

These features make the RNG k- ε model more accurate and reliable for a wider class of flows than the standard k- ε model.

The RNG-based k- ε turbulence model is derived from the instantaneous Navier-Stokes equations, using a mathematical technique called “renormalization group” (RNG) methods. The analytical derivation results in a model with constants different from those in the standard k- ε model, and additional terms and functions in the transport equations for k and ε .

3.5.2 Transport Equations for the RNG k- ε Model

The RNG k- ε model has a similar form to the standard k- ε model:

$$\frac{\partial}{\partial t}(\rho k) + \frac{\partial}{\partial x_j}(\rho k u_j) = \frac{\partial}{\partial x_j} \left(\alpha_k \mu_{\text{eff}} \frac{\partial k}{\partial x_j} \right) + G_k + G_b - \rho \epsilon - Y_M + S_k$$

and

$$\frac{\partial}{\partial t}(\rho \epsilon) + \frac{\partial}{\partial x_j}(\rho \epsilon u_j) = \frac{\partial}{\partial x_j} \left(\alpha_\epsilon \mu_{\text{eff}} \frac{\partial \epsilon}{\partial x_j} \right) + C_{1\epsilon} \frac{\epsilon}{k} (G_k + C_{3\epsilon} G_b) - C_{2\epsilon} \rho \frac{\epsilon^2}{k} - R_\epsilon + S_\epsilon$$

In these equations, G_k represents the generation of turbulence kinetic energy due to the mean velocity gradients. G_b is the generation of turbulence kinetic energy due to buoyancy. Y_M represents the contribution of the fluctuating dilatation in compressible turbulence to the overall dissipation rate.

3.5.3 Modeling the Effective Viscosity

The scale elimination procedure in RNG theory results in a differential equation for turbulent viscosity:

$$d \left(\frac{\rho^2 k}{\sqrt{\epsilon \mu}} \right) = 1.72 \frac{\hat{\nu}}{\sqrt{\hat{\nu}^3 - 1 + C_\nu}} d\hat{\nu}$$

where

$$\begin{aligned} \hat{\nu} &= \mu_{\text{eff}} / \mu \\ C_\nu &\approx 100 \end{aligned}$$

Equation above is integrated to obtain an accurate description of how the effective turbulent transport varies with the effective Reynolds number (or eddy scale), allowing

the model to better handle low-Reynolds-number and near-wall flows. In the high-Reynolds-number limit, Equation 10.4-6 gives

$$\mu_t = \rho C_\mu \frac{k^2}{\epsilon}$$

with $C_\mu = 0.0845$, derived using RNG theory. It is interesting to note that this value of C_μ is very close to the empirically-determined value of 0.09 used in the standard k- ϵ model.

In FLUENT, by default, the effective viscosity is computed using the high-Reynolds number form in equation above.

3.5.4 RNG Swirl Modification

Turbulence, in general, is affected by rotation or swirl in the mean flow. The RNG model in FLUENT provides an option to account for the effects of swirl or rotation by modifying the turbulent viscosity appropriately. The modification takes the following functional form:

$$\mu_t = \mu_{t0} f\left(\alpha_s, \Omega, \frac{k}{\epsilon}\right)$$

Where μ_{t0} is the value of turbulent viscosity calculated without the swirl modification. Ω is a characteristic swirl number evaluated within FLUENT, and α_s is a swirl constant that assumes different values depending on whether the flow is swirl-dominated or only mildly swirling. This swirl modification always takes effect for axisymmetric, swirling flows and three-dimensional flows when the RNG model is selected. For mildly swirling flows (the default in FLUENT), α_s is set to 0.05 and cannot be modified. For strong swirling flows, however, a higher value of α_s can be used.

3.5.5 Calculating the Inverse Effective Prandtl Numbers

The inverse effective Prandtl numbers, α_k and α_θ , are computed using the following formula derived analytically by the RNG theory:

$$\left| \frac{\alpha - 1.3929}{\alpha_0 - 1.3929} \right|^{0.6321} \left| \frac{\alpha + 2.3929}{\alpha_0 + 2.3929} \right|^{0.3679} = \frac{\mu_{mol}}{\mu_{eff}}$$

where $\alpha_0 = 1.0$. In the high-Reynolds-number limit ($\mu_{mol}/\mu_{eff} \leq 1$), $\alpha_k = \alpha_\theta = 1.393$.

RNG model is more responsive to the effects of rapid strain and streamline curvature than the standard k- ϵ model, which explains the superior performance of the RNG model for certain classes of flows.

3.6 Area and Diameter Calculation for FLUENT input

Collector or absorber is usually flat or corrugated plate. The corrugated area, A_c is calculated from flat area, A_f

$$\text{Corrugated plate area, } A_c = \pi/2 \times \text{Flat plate area, } A_f = 1.57 \times A_f$$

Where

$$A_f = \text{width} \times \text{length}$$

$$\text{Hydraulic diameter, } D_h = 4A / P$$

Where

$$A = \text{Area} = \text{width} \times \text{length}$$

$$P = 2 (A)$$

CHAPTER 4

METHODOLOGY

4.1 Tools

CFD software that used to accomplished the project objectives are;

- i) GAMBIT software
- ii) FLUENT software

4.2 Technique of Analysis

CFD simulation is done to get better result on the air flow inside and outside the chimney and to improve the electricity generation. The parameters required in simulation are such as dimension of the design, temperature of collector and cover, intensity of solar radiation, pressure or velocity inlet of the chimney. Navier-Stokes, mass and energy conservation equation governing the fluid flow will be involved in simulation. The numerical simulation of air movement in solar chimney will produce the result on velocity and temperature of solar chimney outlet. The expected outputs from simulation are distribution of pressure, temperature and velocity of chimney inlet. The simulation is expected to be applied for solar - biomass integration system too.

From the GAMBIT software, 2D or 3D drawing is produced. The desired drawing is drawn in coordinate system. The design drawing is started with vertex, edge and finalized with face formation or straight choose volume. Later, the 2D or 3D drawing is meshed with required information and later the file will be exported to FLUENT software. In the FLUENT, all the value of properties of the fluid and the surrounding of it is entered inside. The graph plot and contour display is used to view the output. As a result, the velocity, pressure, temperature distribution pattern, the skin friction coefficient manipulation and other criteria is observed using the CFD software.

Since this project need is to find the suitable parameter to optimize the electricity generation by obtaining higher outlet velocity from chimney, several drawing and simulation are brainstormed. And all the drawing will be analyzed using the CFD simulation. Once the satisfied value is obtained, further action will be taken after consultation with this project supervisor.

4.3 Procedures

The analysis is done for three cases with different configurations. Below shown are the cases to be investigated. Each configuration is drawn in GAMBIT as 2D drawing and run in FLUENT software.

Table 4.1- Case 1 to be investigated

<i>Case 1</i>	Configuration 1	Option A
		Option B
	Configuration 2	Option A
		Option B

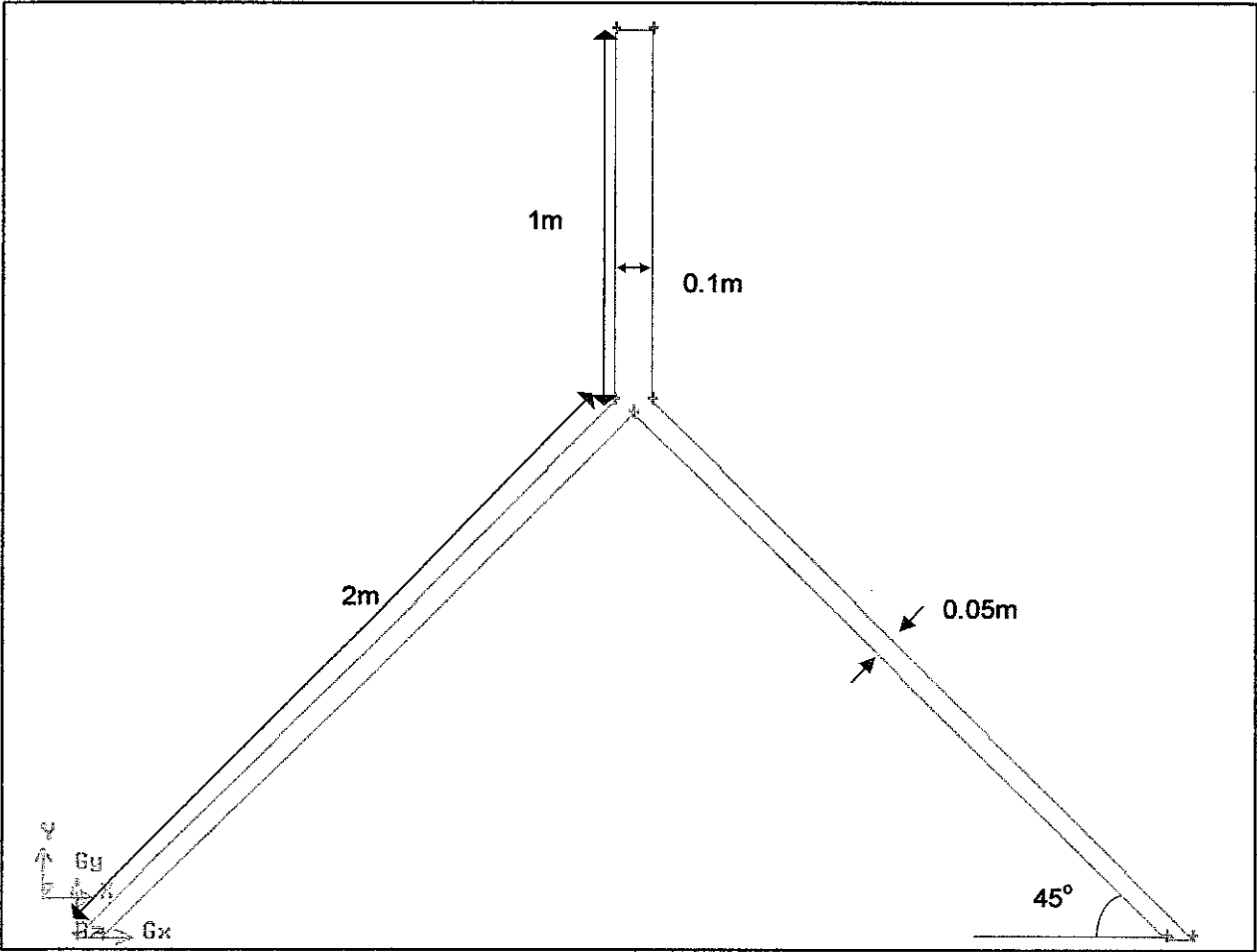
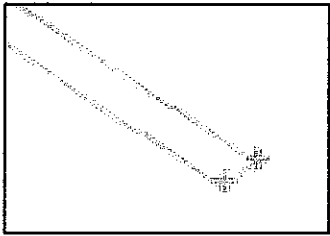
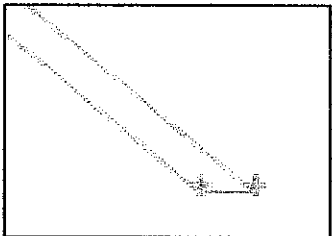


Figure 4.1-Dimension of the roof and chimney drawing for case 1



Inlet configuration 1



Inlet configuration 2

Table 4.2-Case 2 to be investigated

<i>Case 2</i>	Configuration 3	Collector Temperature	a) $D_{in} = 0.050m$
			b) $D_{in} = 0.057m$
			c) $D_{in} = 0.100m$
		Convection	a) $D_{in} = 0.050m$
			b) $D_{in} = 0.057m$
			c) $D_{in} = 0.100m$
	Configuration 4	Collector Temperature	a) $D_{in} = 0.0707m$
			b) $D_{in} = 0.0806m$
			c) $D_{in} = 0.1414m$
		Convection	a) $D_{in} = 0.0707m$
			b) $D_{in} = 0.0806m$
			c) $D_{in} = 0.1414m$

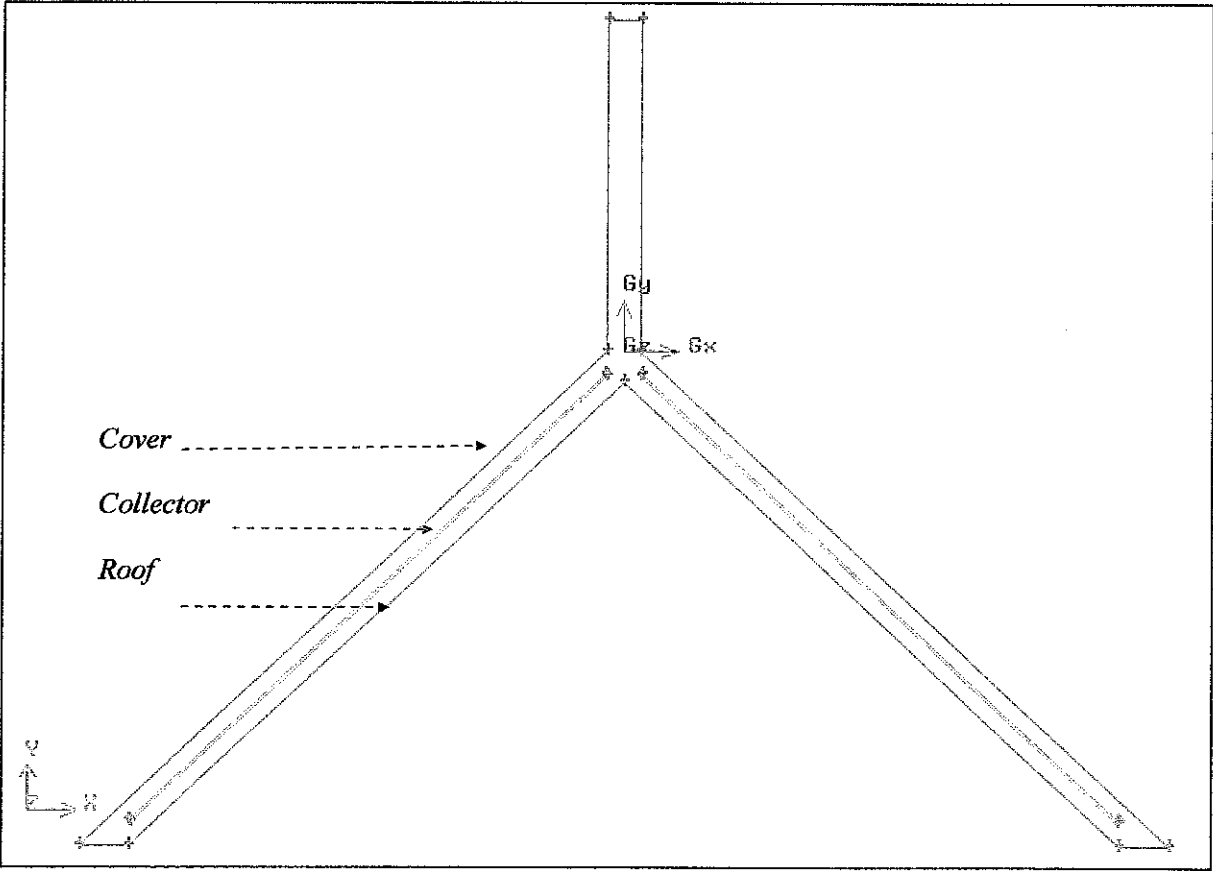


Figure 4.2-GAMBIT drawing for case 2

Table 4.3-Case 3 to be investigated

<i>Case 3</i>	Configuration 5
	Configuration 6

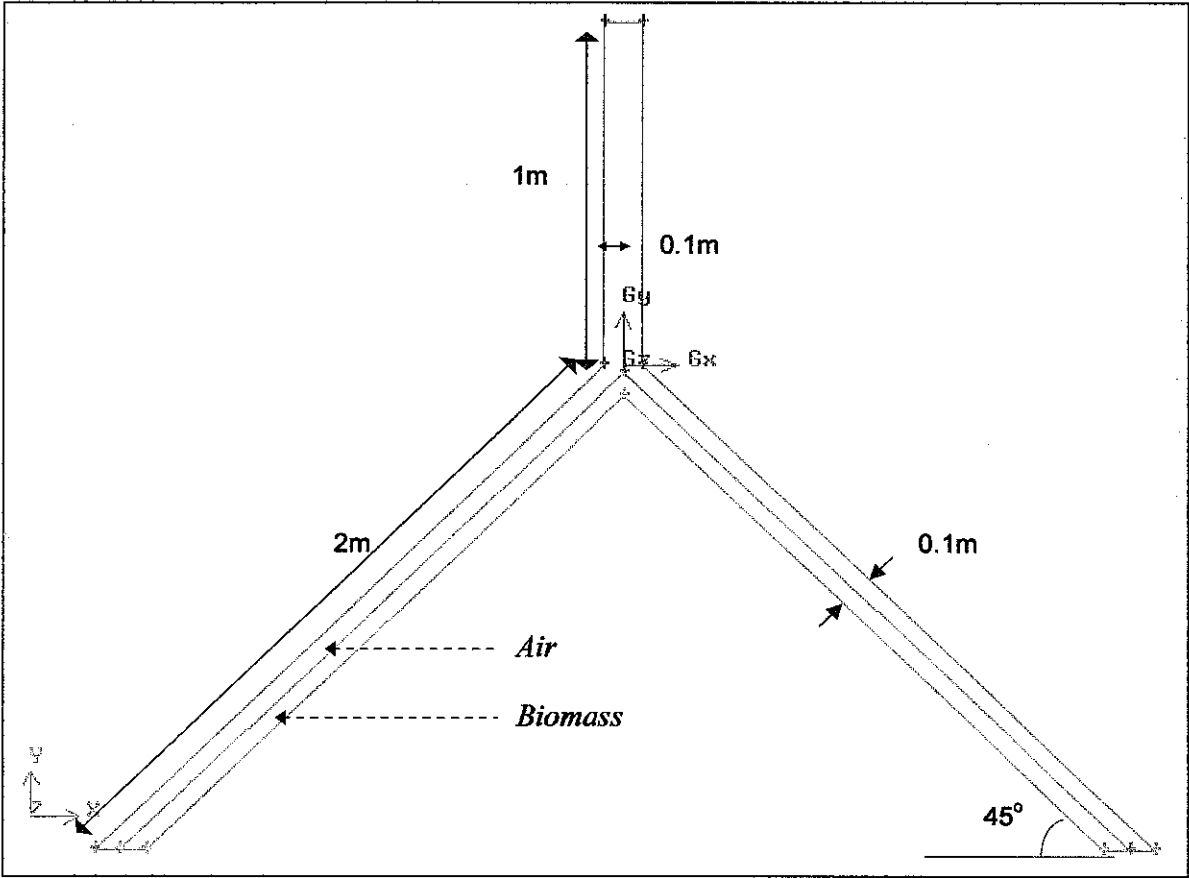


Figure 4.3-Dimension of the roof and chimney drawing for case 3

Table 4.4-Terms description for each configuration

<i>Term</i>	<i>Description</i>	<i>Collector position</i>
Configuration 1	Trimmed inlet with 1 surface contact of collector	On the roof
Configuration 2	Flat inlet 1 surface contact of collector	On the roof

Configuration 3	Trimmed inlet with 2 side of collector surface contact	In between canopy and roof
Configuration 4	Flat inlet with 2 side of collector surface contact	In between canopy and roof
Configuration 5	2 trimmed inlet (air and biomass)	In between air and biomass flow
Configuration 6	2 flat inlet (air and biomass)	In between air and biomass flow
Option A	Same temperature for left and right side of roof	-
Option B	Different temperature for left and right side of roof	-

Table 4.5 - Option A and Option B details

Option A		Option B	
Ambient temperature	31°C	Ambient temperature	31°C
Canopy temperature	80°C	Right canopy temperature	80°C
		Left canopy temperature	67°C
Collector temperature	53°C	Right collector temperature	53°C
		Left collector temperature	49°C

Table 4.6-Materials used in solar chimney system

Item	Collector	Cover	Flow Medium
Material	Aluminum	Perspek (Glass)	Air

4.4 Work Flow Execution

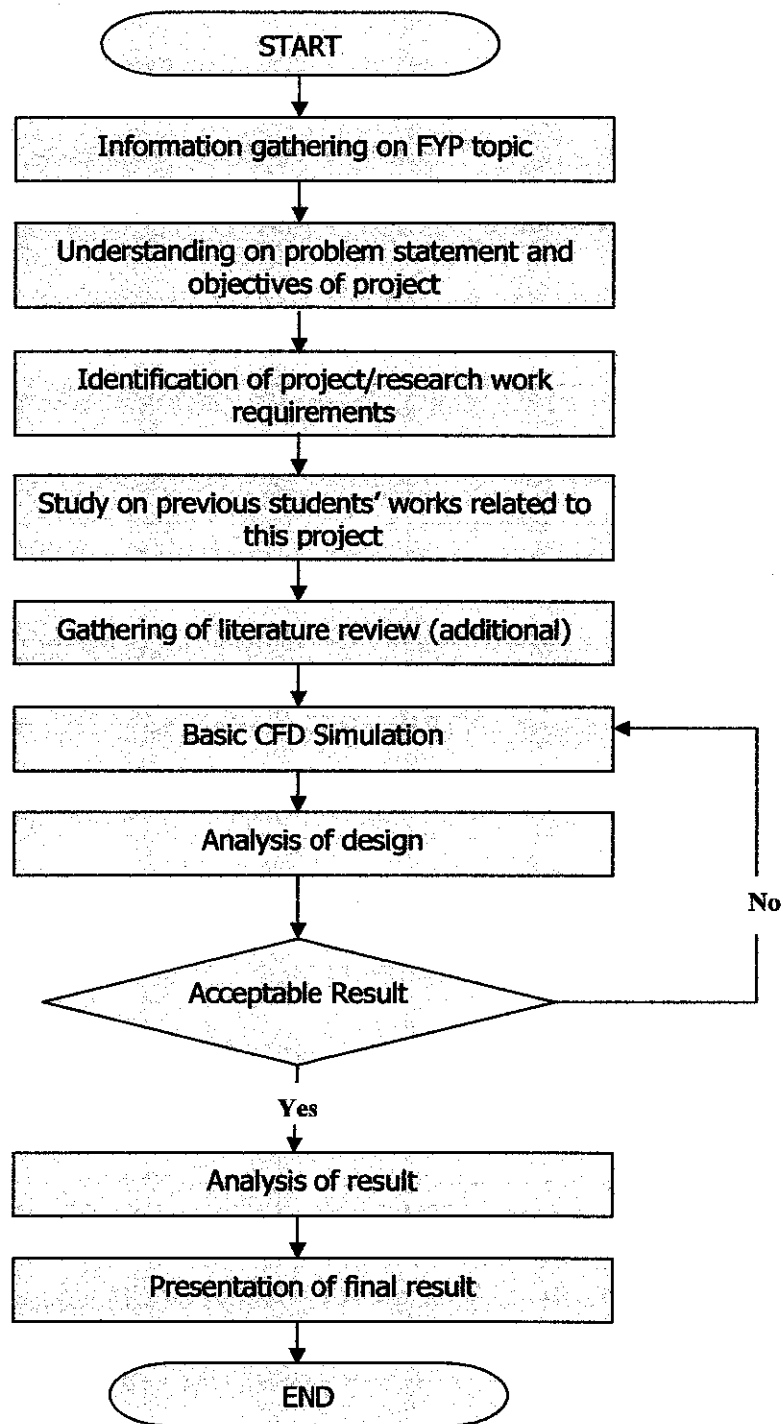


Figure 4.4-Work Flow Chart

4.5 Gantt Chart

Table 4.7 - Schedule for First Semester of Final Year Project (FYP I)

No.	Detail/ Week	1	2	3	4	5	6	7	8	9	10	11	12	13	14	SW	EW
1	Submission of Topic Proposal																
2	Preliminary Research Work																
3	Introduction to GAMBIT and FLUENT																
4	Identification of project work flow																
5	Submission of Preliminary Report																
6	Familiarization to GAMBIT and FLUENT																
7	Find and understand Literature Review																
8	Submission of Literature Review Report																
9	Submission of Progress Report																
10	Seminar																
11	GAMBIT and FLUENT practices																
12	Basic CFD design and simulation																
13	Submission of Interim Report First Draft																
14	Submission of Interim Report Final Draft																
15	Oral Presentation																

SW – Study Week EW – Exam Week Mid-Semester Break

Table 4.8 - Schedule for Second Semester of Final Year Project (FYP II)

No.	Detail/ Week	1	2	3	4	5	6	7	8	9		10	11	12	13	14
1	Project Work Continue															
2	Submission of Progress Report 1			13/2												
3	Project Work Continue															
4	Submission of Progress Report 2									16/3						
5	Seminar									1/4						
6	Project Work Continue															
7	Poster Exhibition												3/4			
8	Submission of Dissertation (soft bound)													27/4		
9	Oral Presentation														29/5	
10	Submission of Dissertation (hard bound)															4/6



Mid-Semester Break

CHAPTER 5

RESULT & DISCUSSION

5.1 Sample of Fluent Result

5.1.1 Different Inlet Configuration Results

5.1.1.1 Case 1, Configuration 1 - Trimmed Inlet

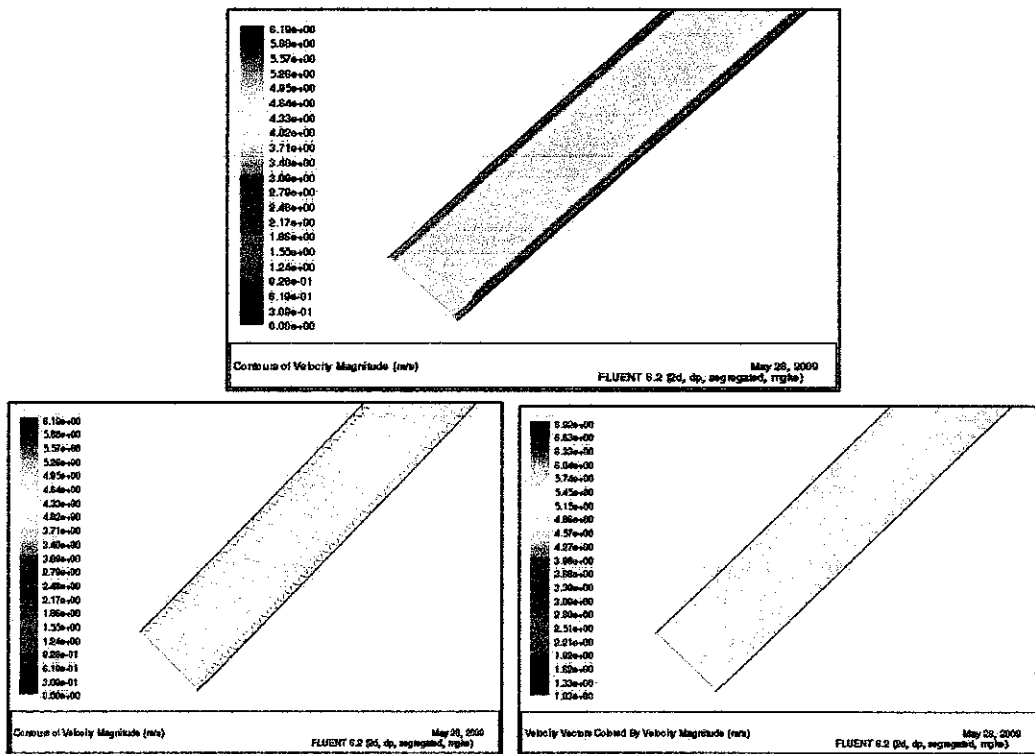


Figure 5.1- Case11A-From top to bottom; left to right:
Velocity Contour, Velocity Contour Mesh, and Velocity Vector

5.1.1.2 Case 1, Configuration 2 – Flat Inlet

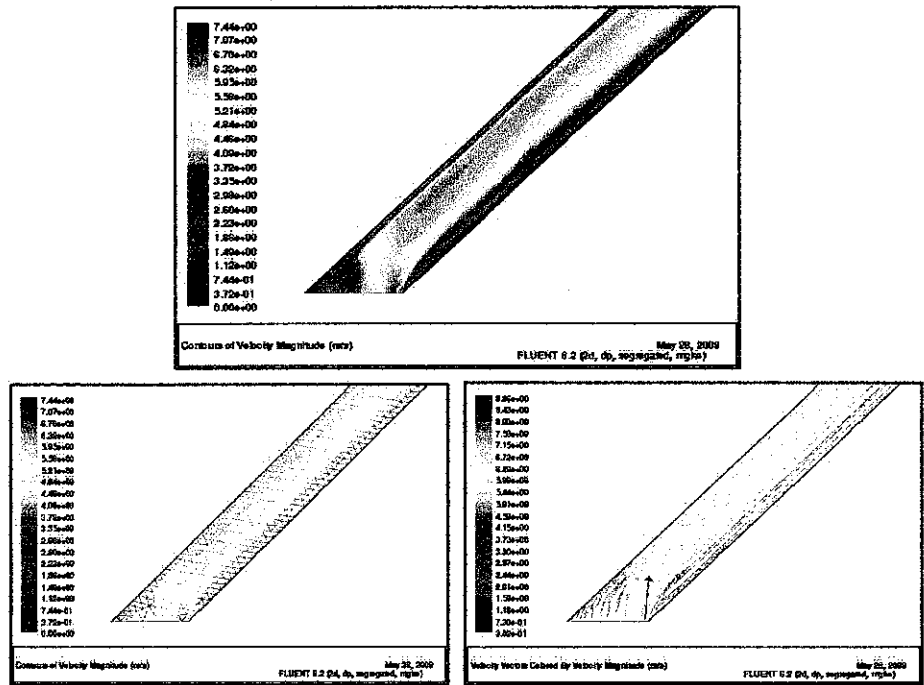


Figure 5.2- Case12A-From top to bottom; left to right:
Velocity Contour, Velocity Contour Mesh, and Velocity Vector

5.1.1.3 Case 2, Configuration 1 - Trimmed Inlet (Convection)

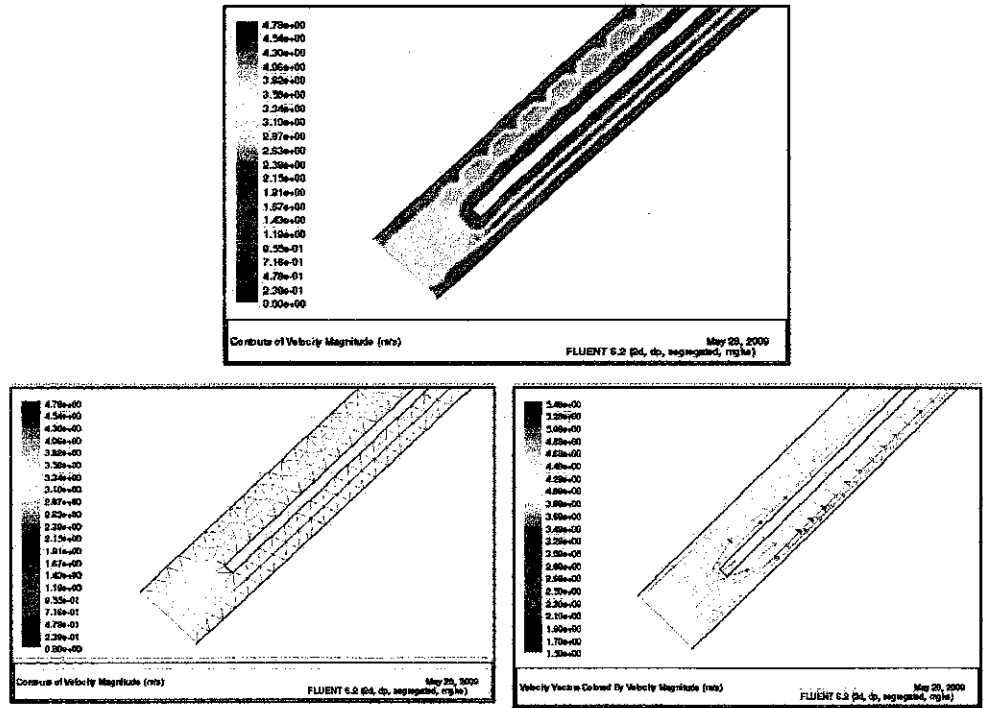


Figure 5.3-Case232-From top to bottom; left to right:
Velocity Contour, Velocity Contour Mesh, and Velocity Vector

5.1.1.4 Case 2, Configuration 2 - Flat Inlet (Convection)

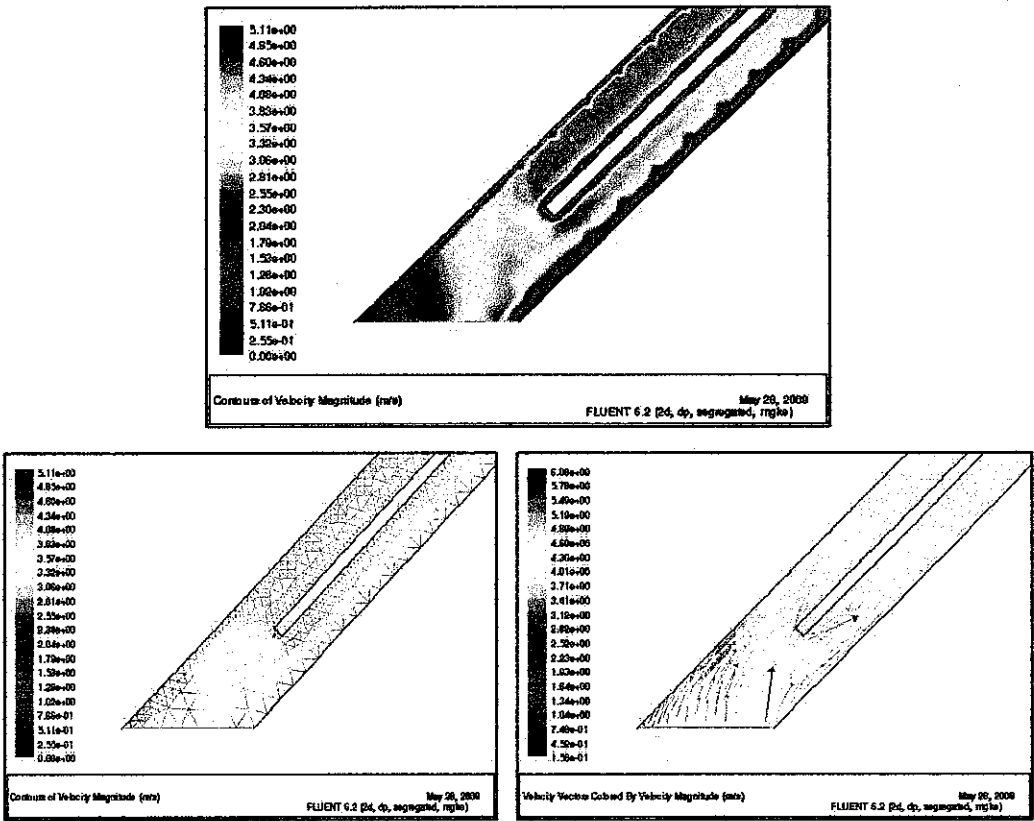


Figure 5.4-Case242-From top to bottom; left to right:
Velocity Contour, Velocity Contour Mesh, and Velocity Vector

5.1.2 Different Case Results

5.1.2.1 Case 1, Configuration 1, Option A

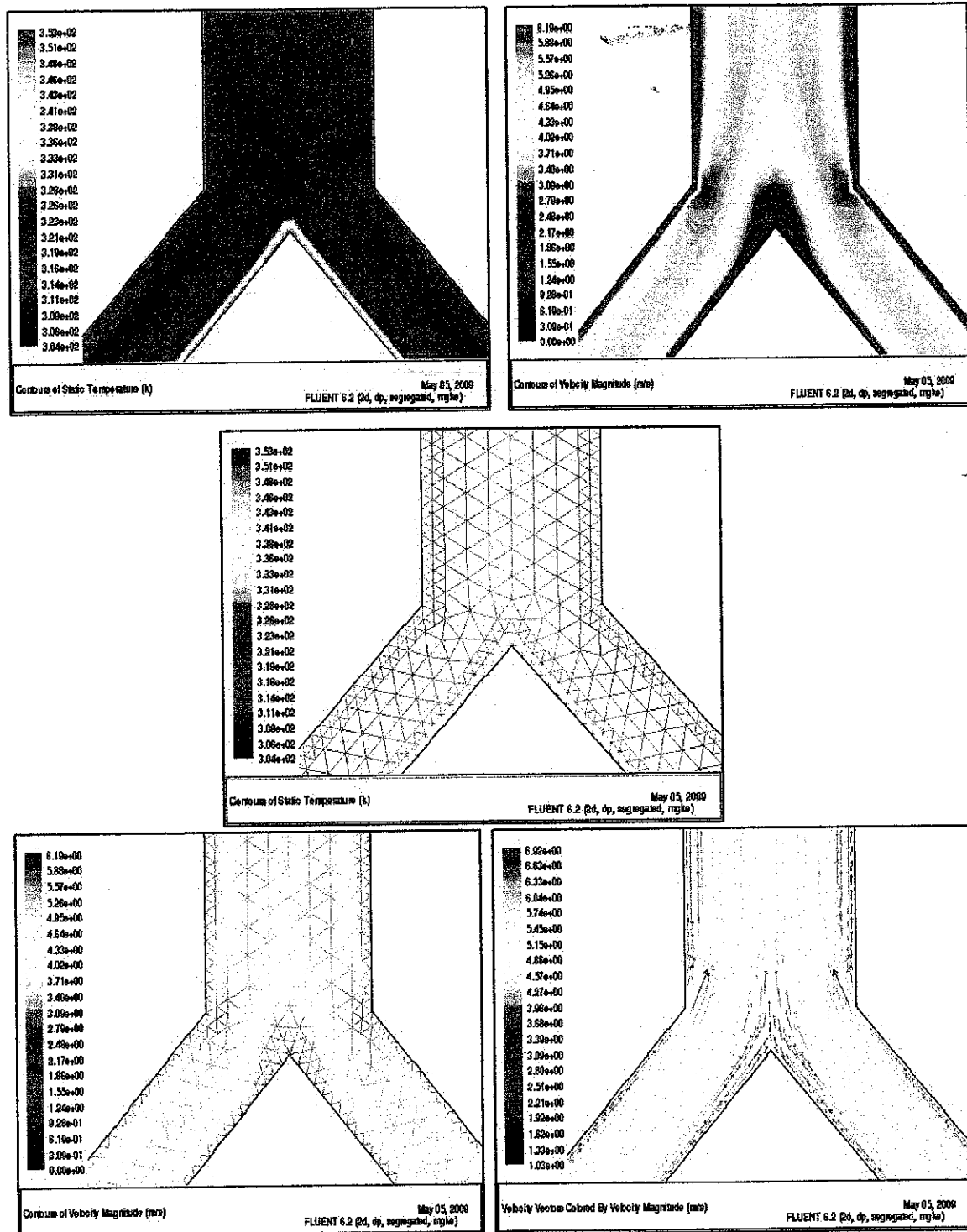


Figure 5.5 -Case 11A-From top to bottom; left to right: Temperature Contour, Velocity Contour, Temperature Contour Mesh, Velocity Contour Mesh, and Velocity Vector

5.1.2.2 Case 2, Configuration 3, Option 1(Collector Temperature)

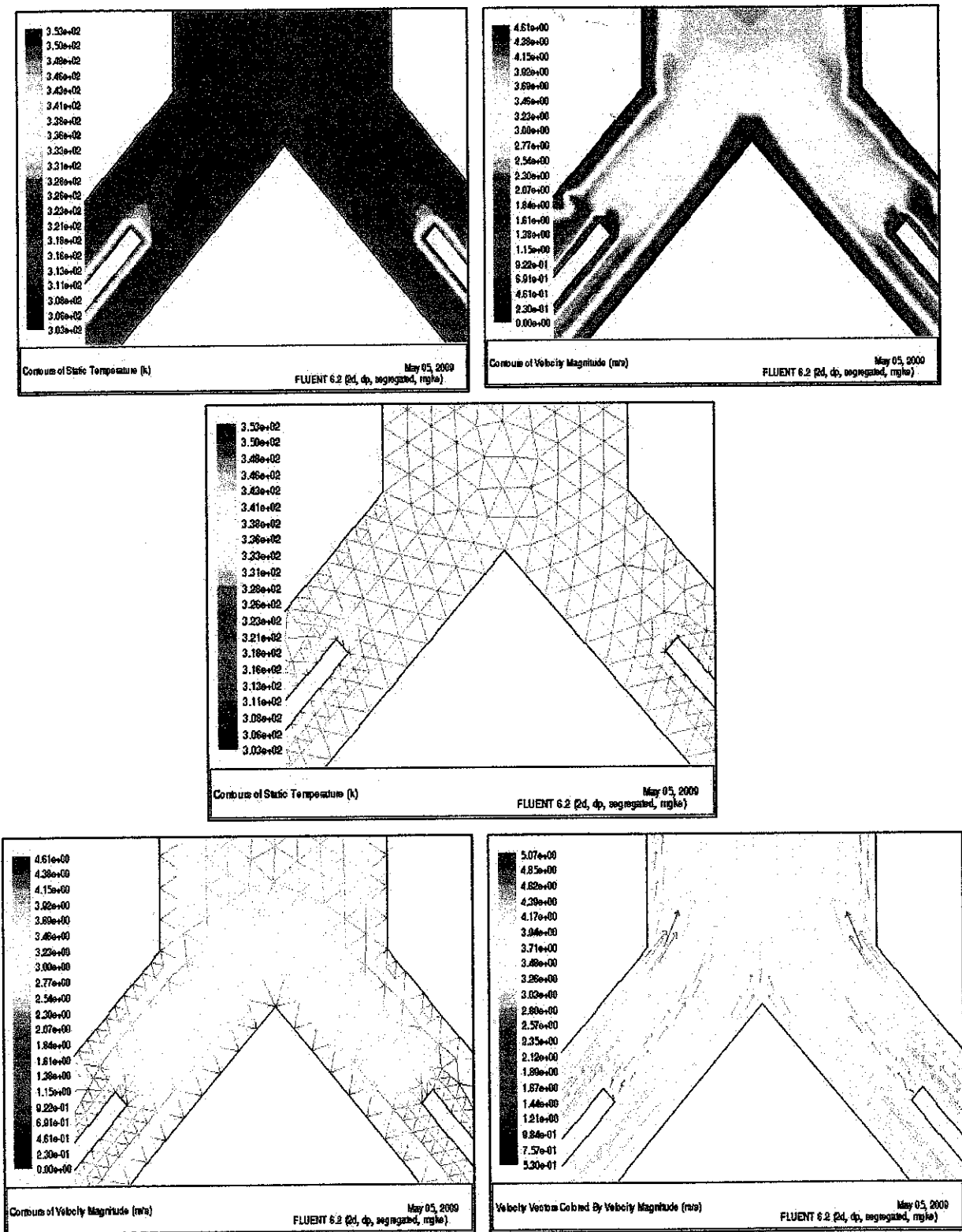


Figure 5.6- Case 2311-From top to bottom; left to right: Temperature Contour, Velocity Contour, Temperature Contour Mesh, Velocity Contour Mesh, and Velocity Vector

5.1.2.3 Case 3, Configuration 5

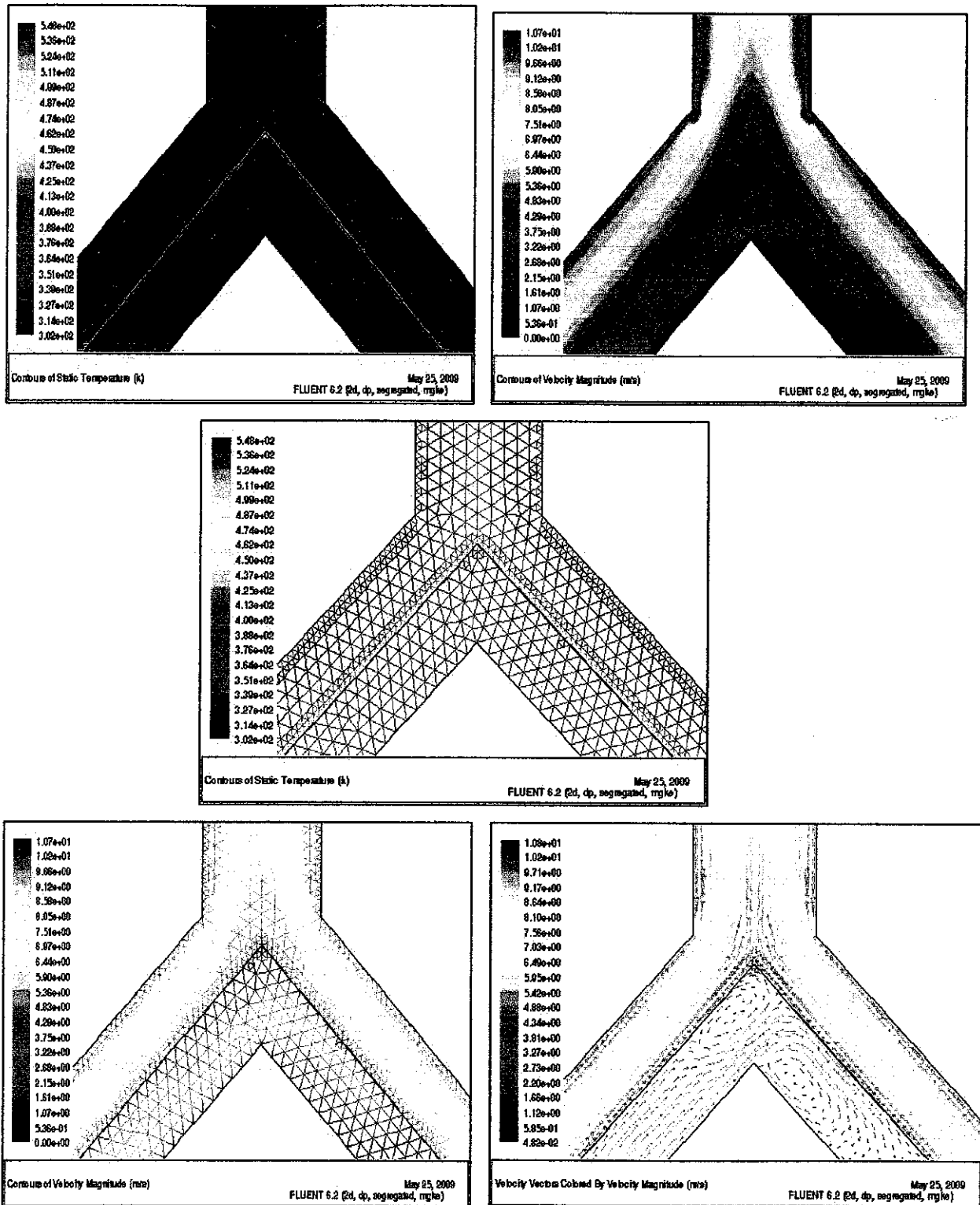
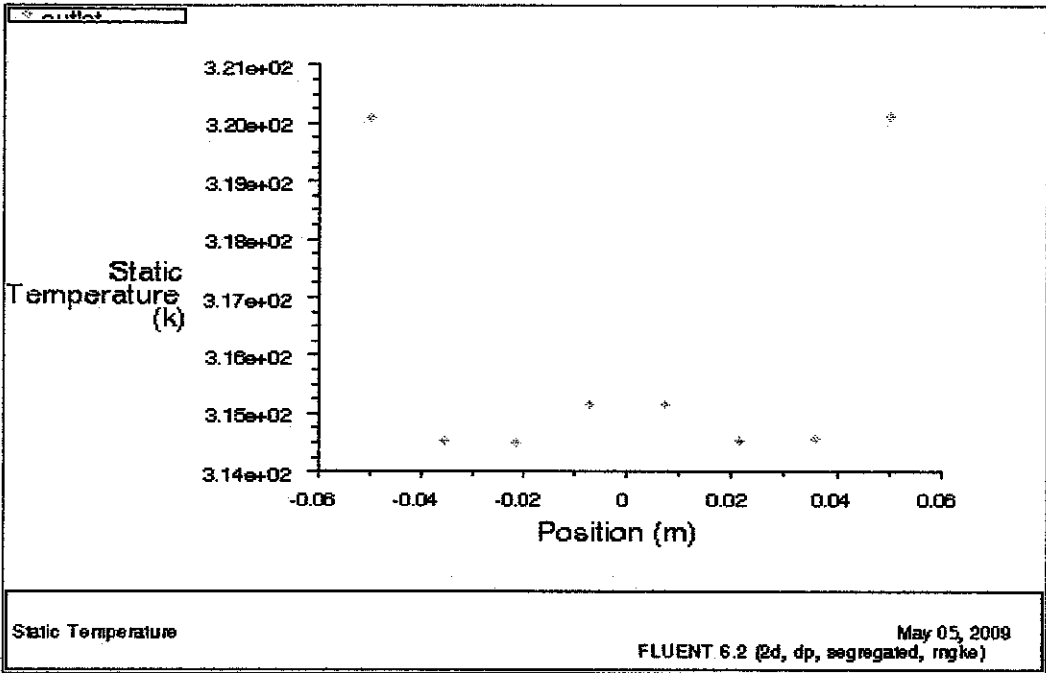


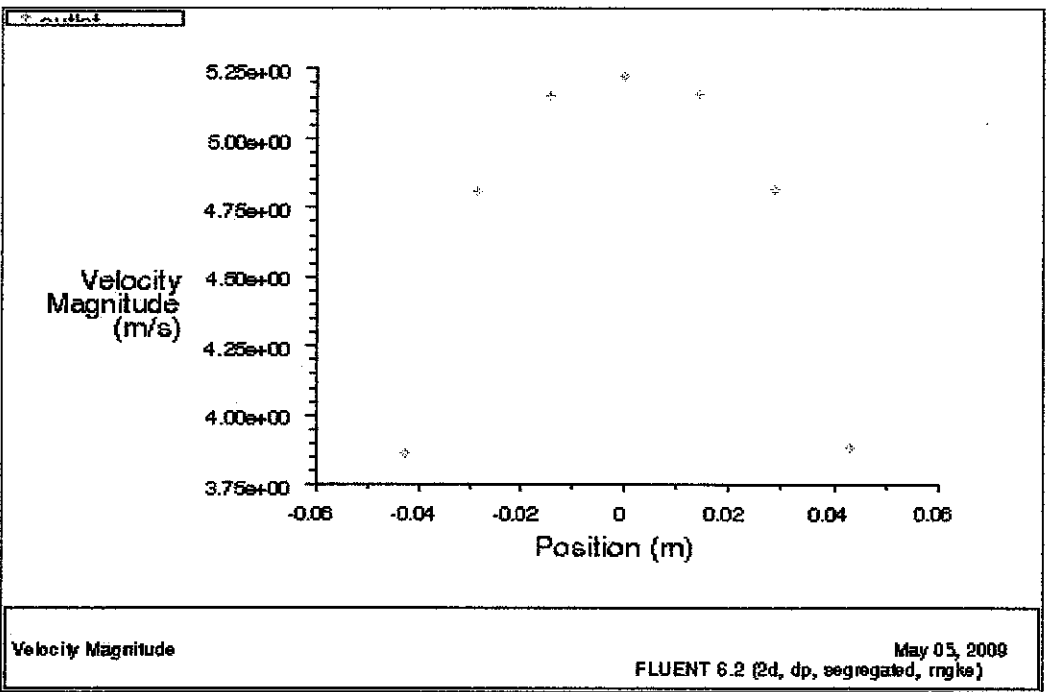
Figure 5.7 - Case35- From top to bottom; left to right: Temperature Contour, Velocity Contour, Temperature Contour Mesh, Velocity Contour Mesh, and Velocity Vector

5.2 Temperature and Velocity Plot

5.2.1 Case 1, Configuration 1, Option A

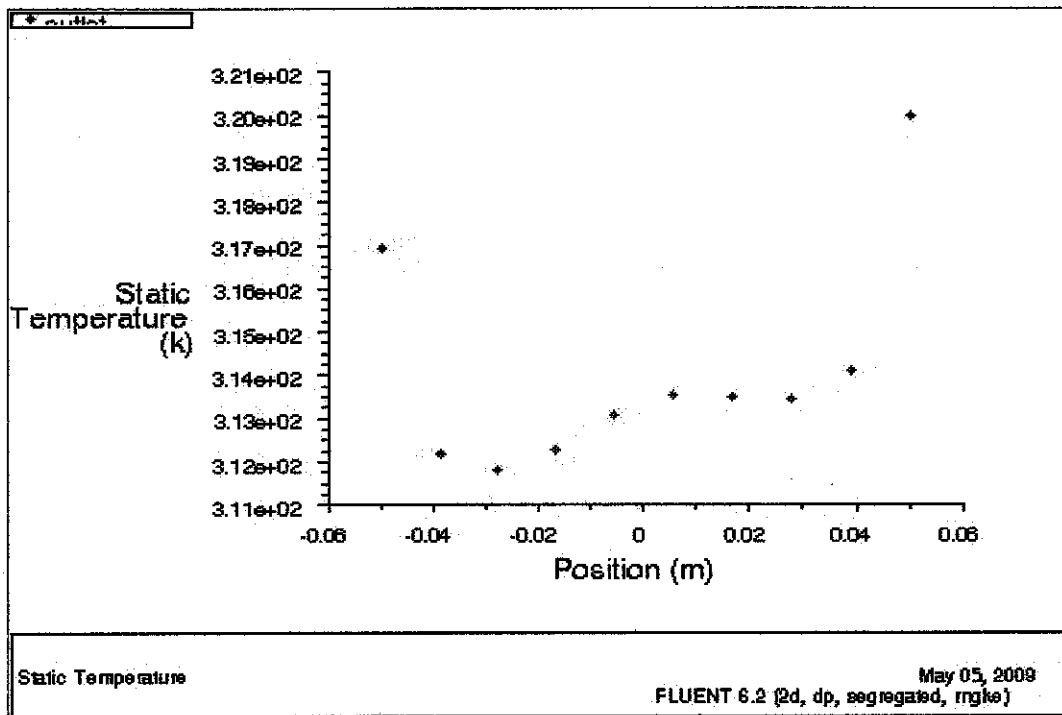


Static Temperature Plot

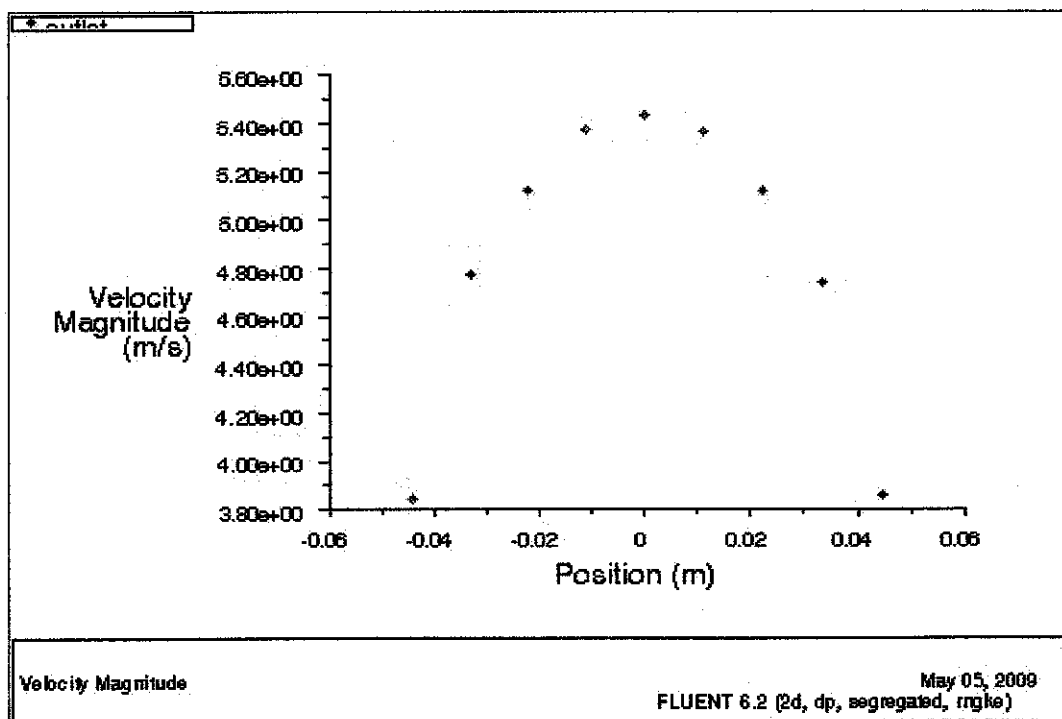


Velocity Magnitude Plot

5.2.2 Case 1, Configuration 1, Option B

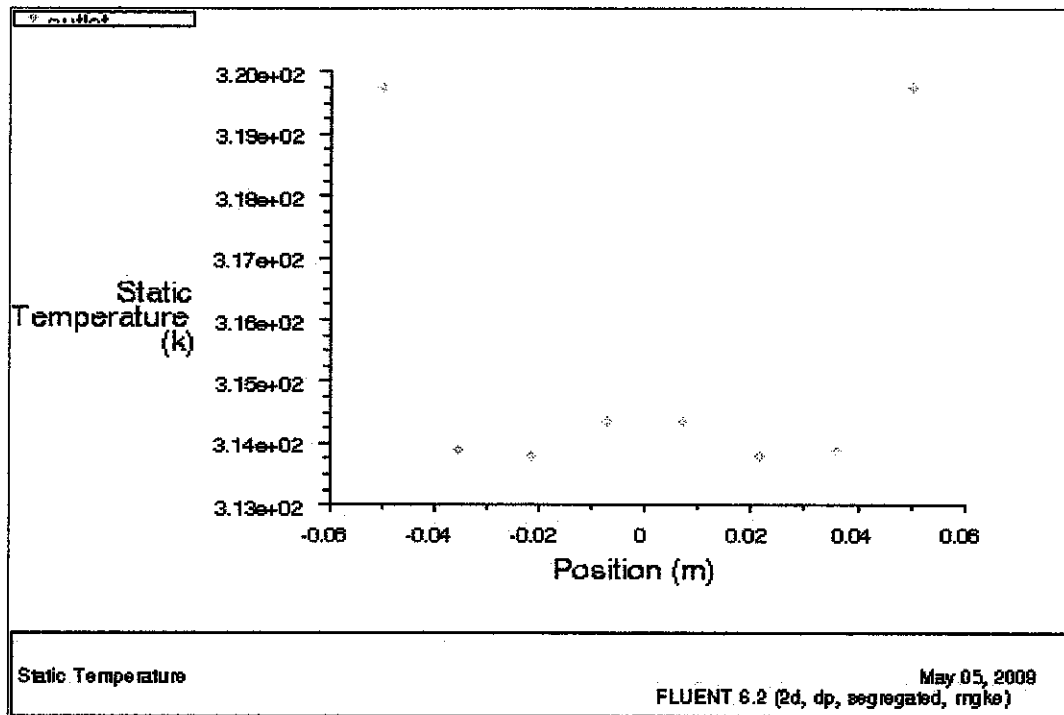


Static Temperature Plot

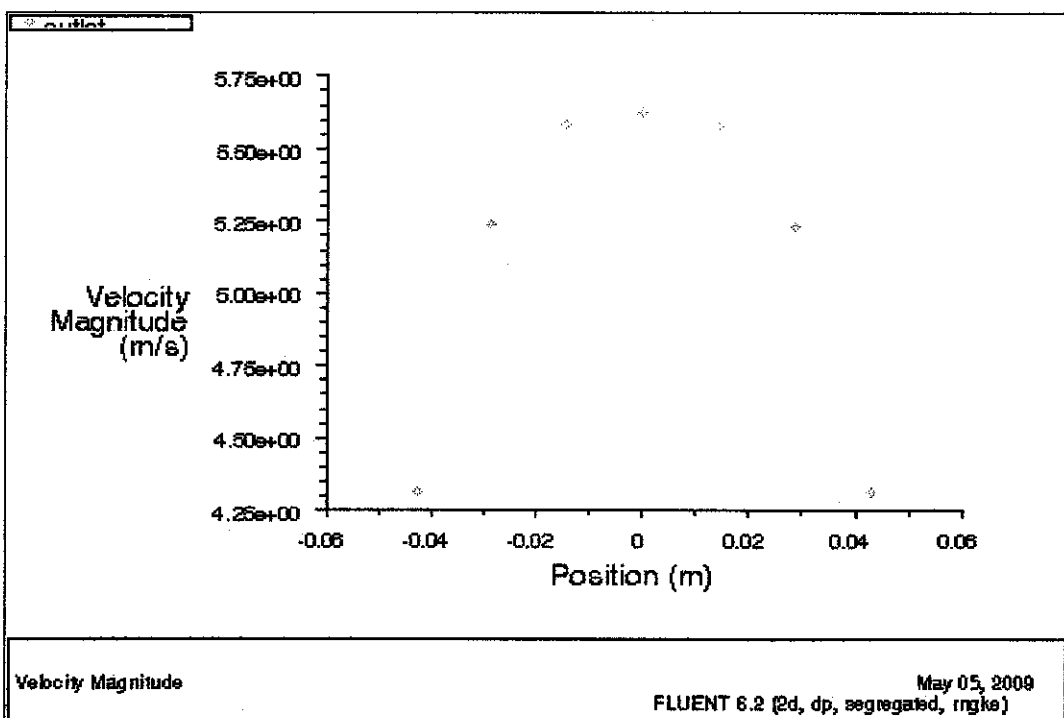


Velocity Magnitude Plot

5.2.3 Case 1, Configuration 2, Option A

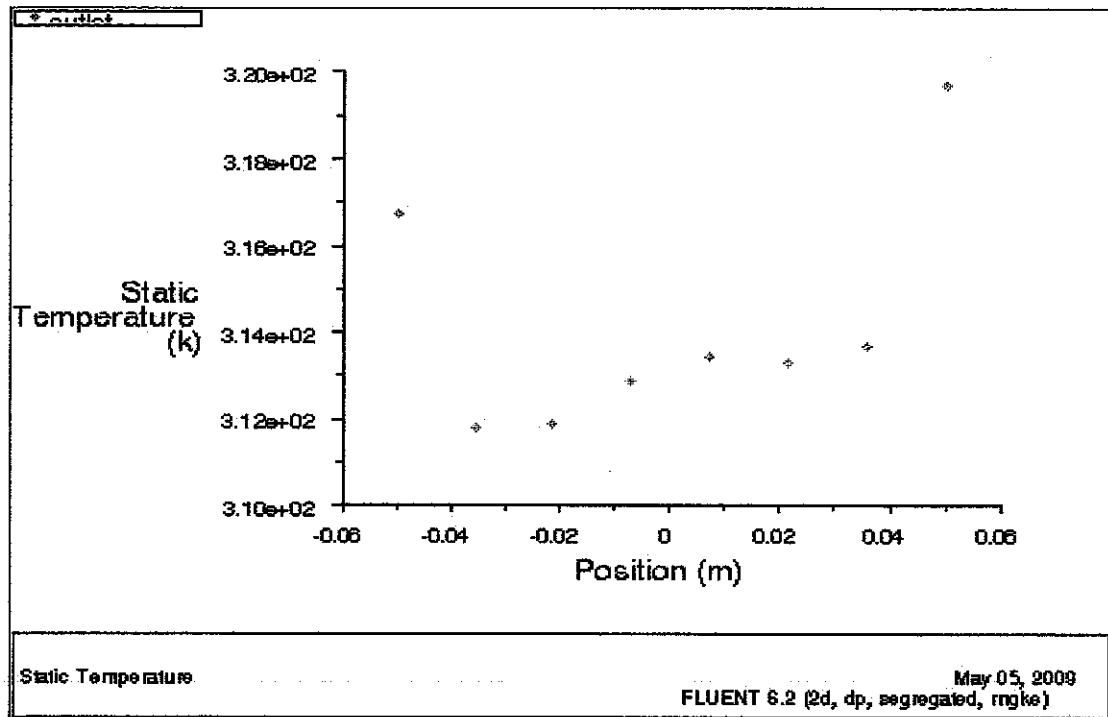


Static Temperature Plot

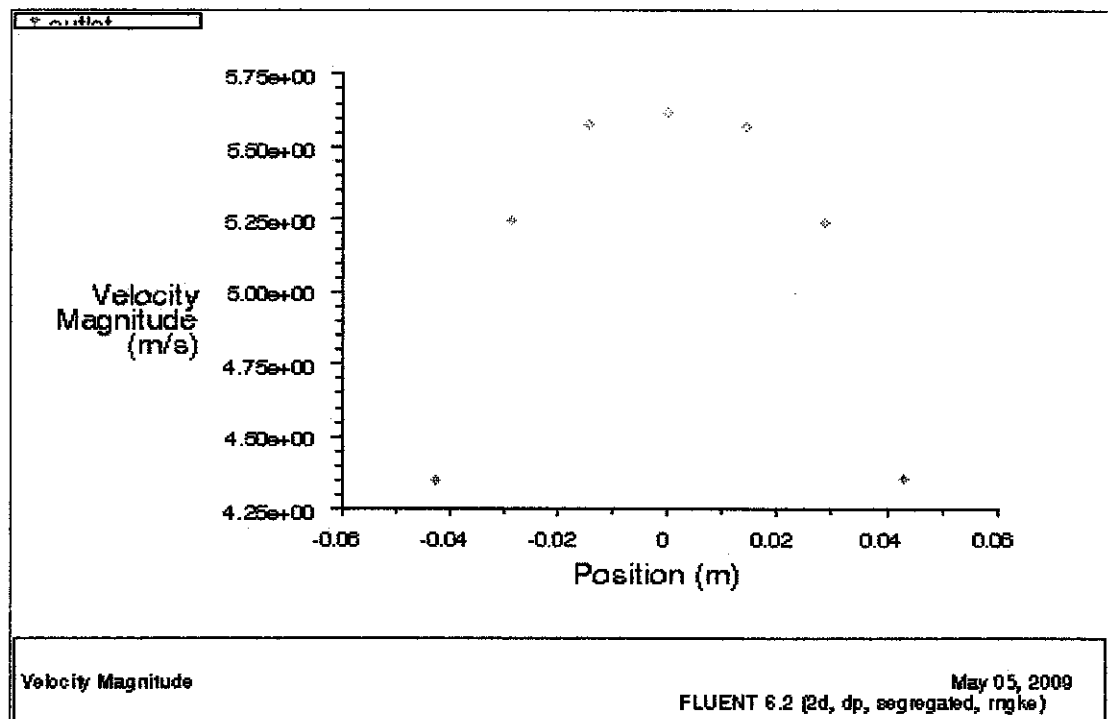


Velocity Magnitude Plot

5.2.4 Case 1, Configuration 2, Option B

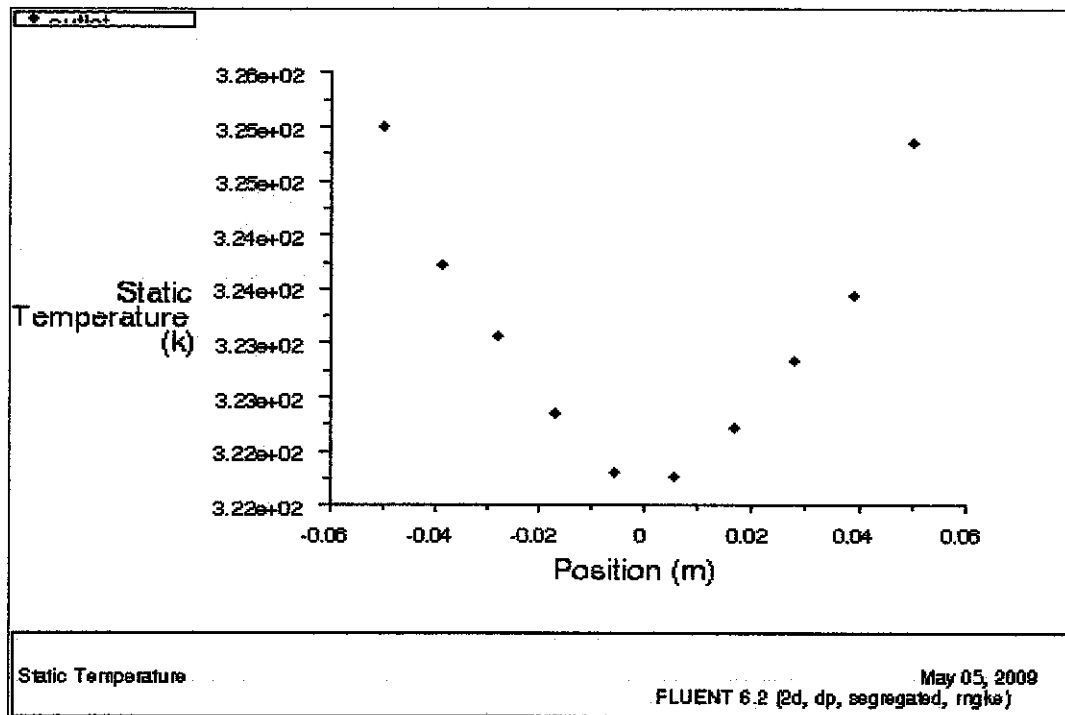


Static Temperature Plot

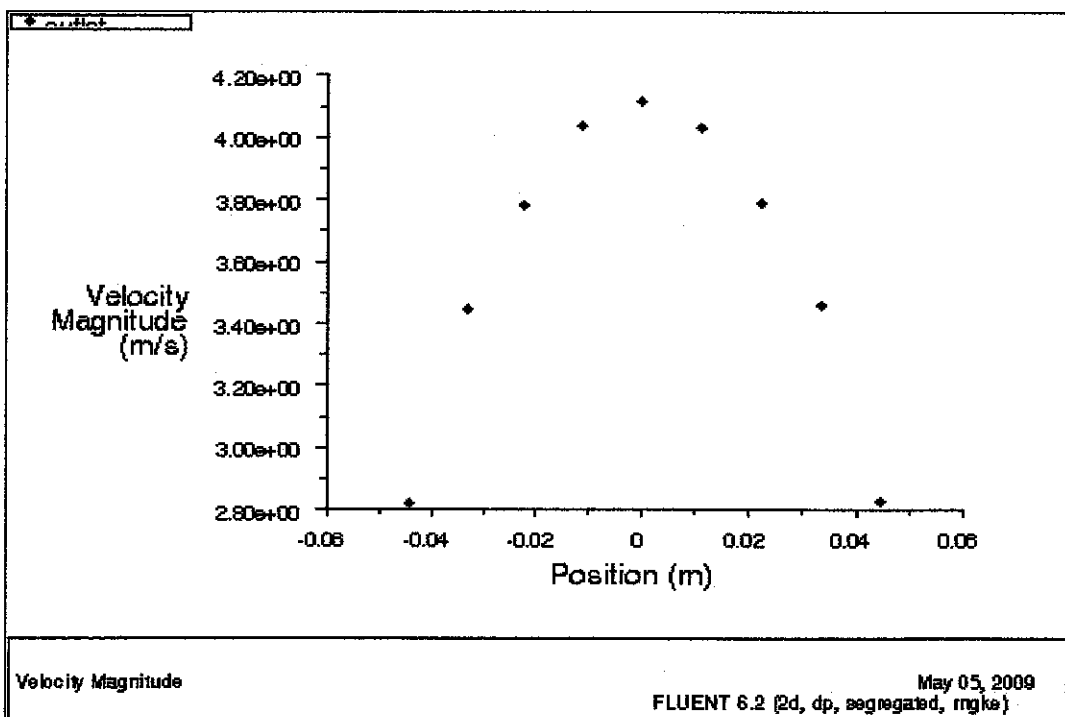


Velocity Magnitude Plot

5.2.5 Case 2, Configuration 3, Option 1a

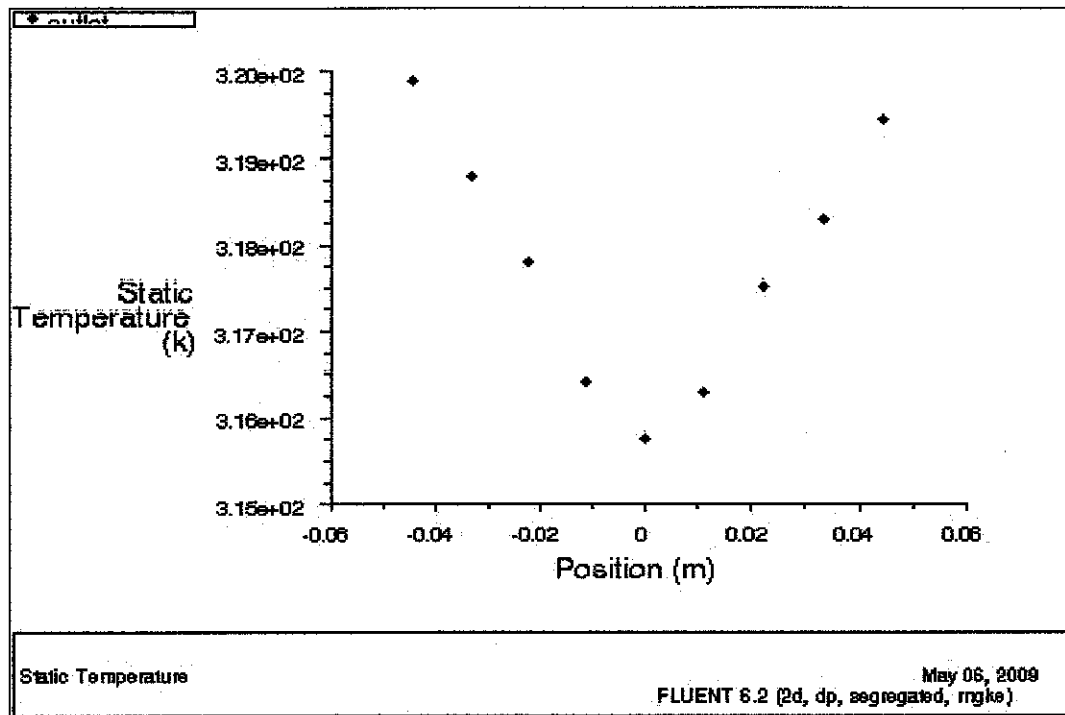


Static Temperature Plot

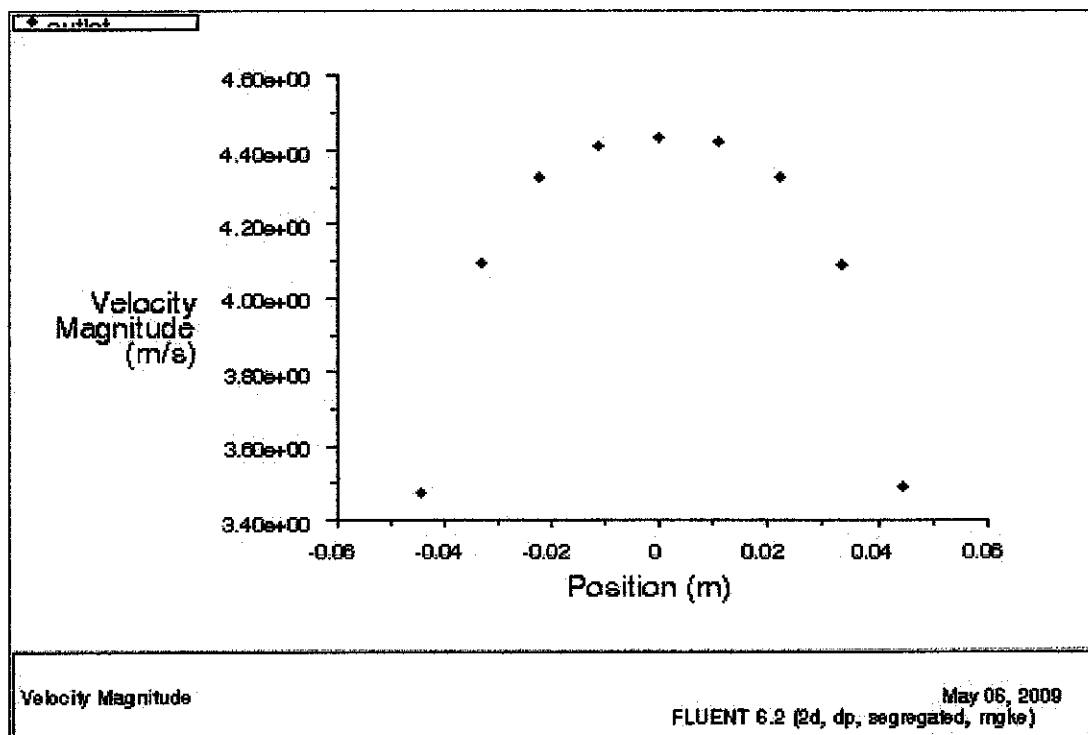


Velocity Magnitude Plot

5.2.6 Case 2, Configuration 3, Option 1b

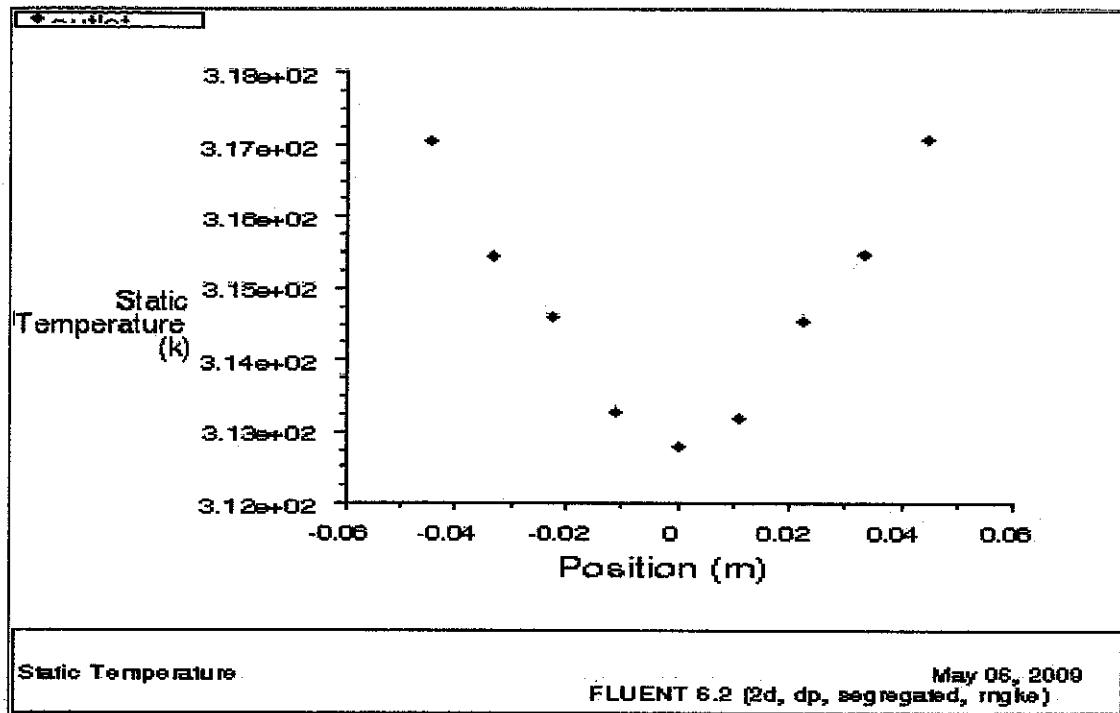


Static Temperature Plot

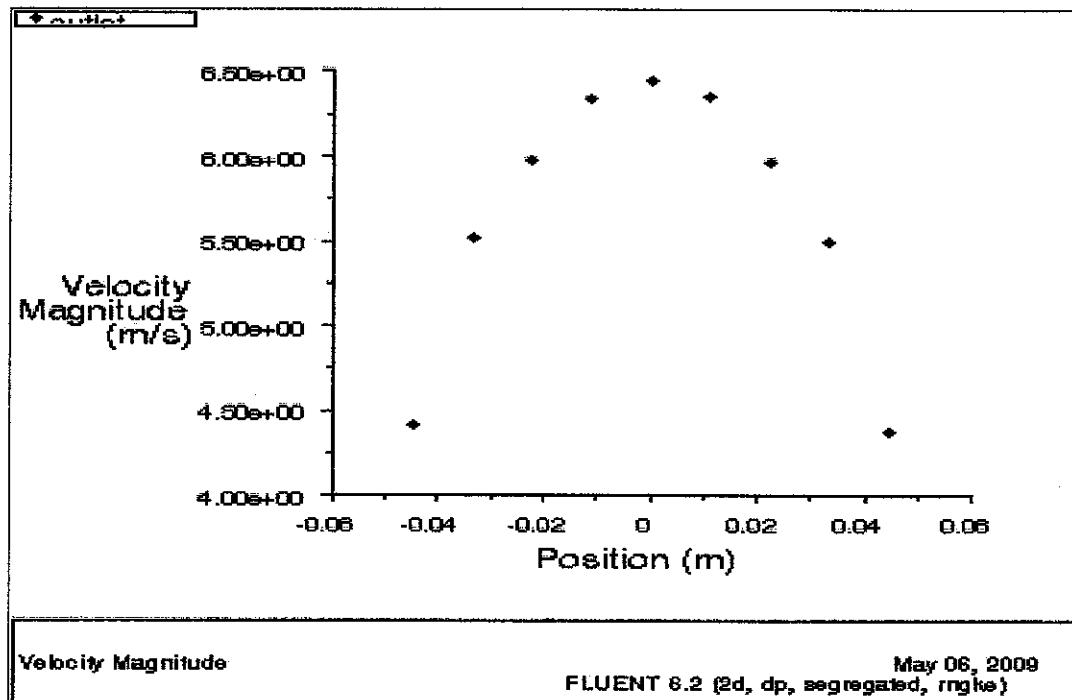


Velocity Magnitude Plot

5.2.7 Case 2, Configuration 3, Option 1c

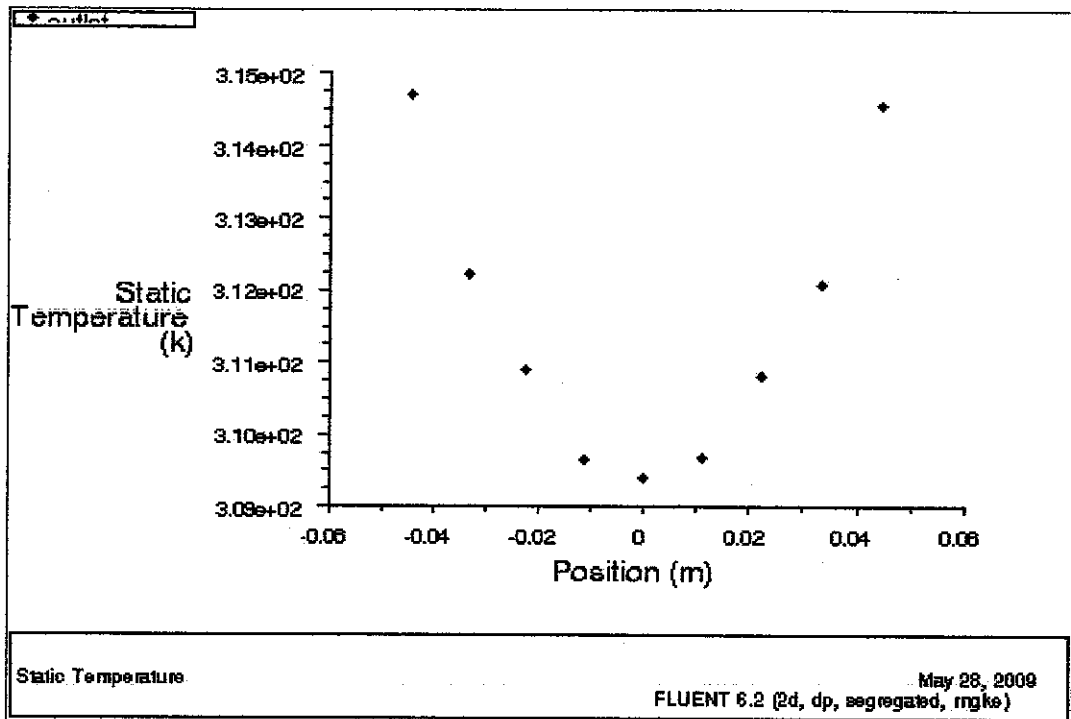


Static Temperature Plot

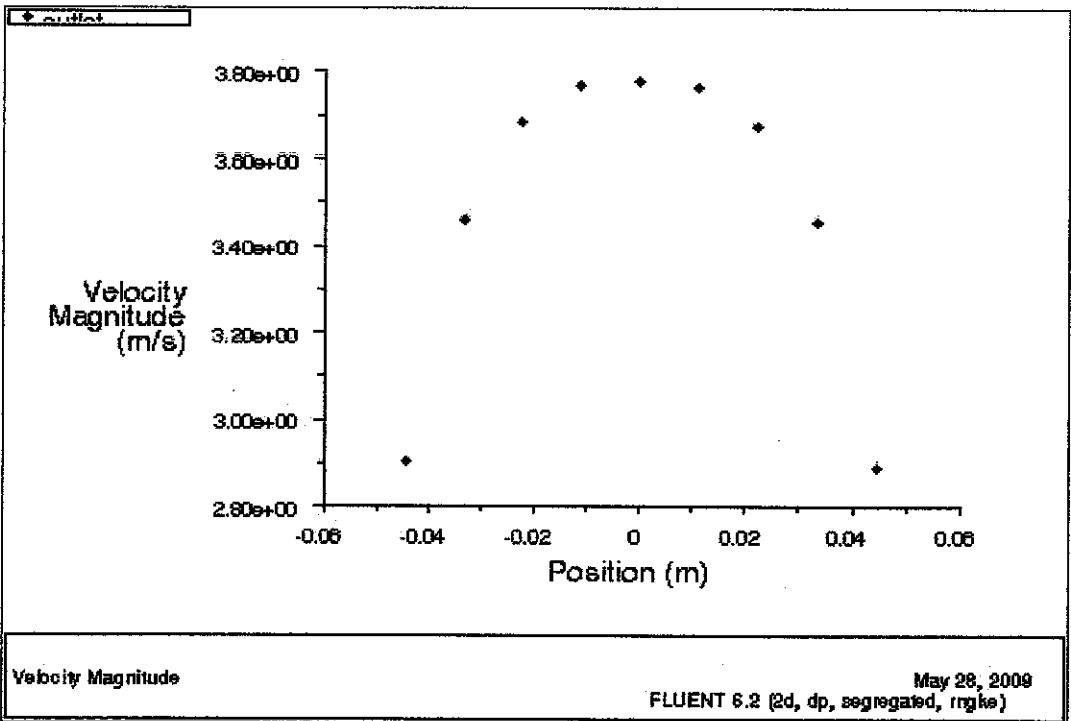


Velocity Magnitude Plot

5.2.8 Case 2, Configuration 3, Option 2a

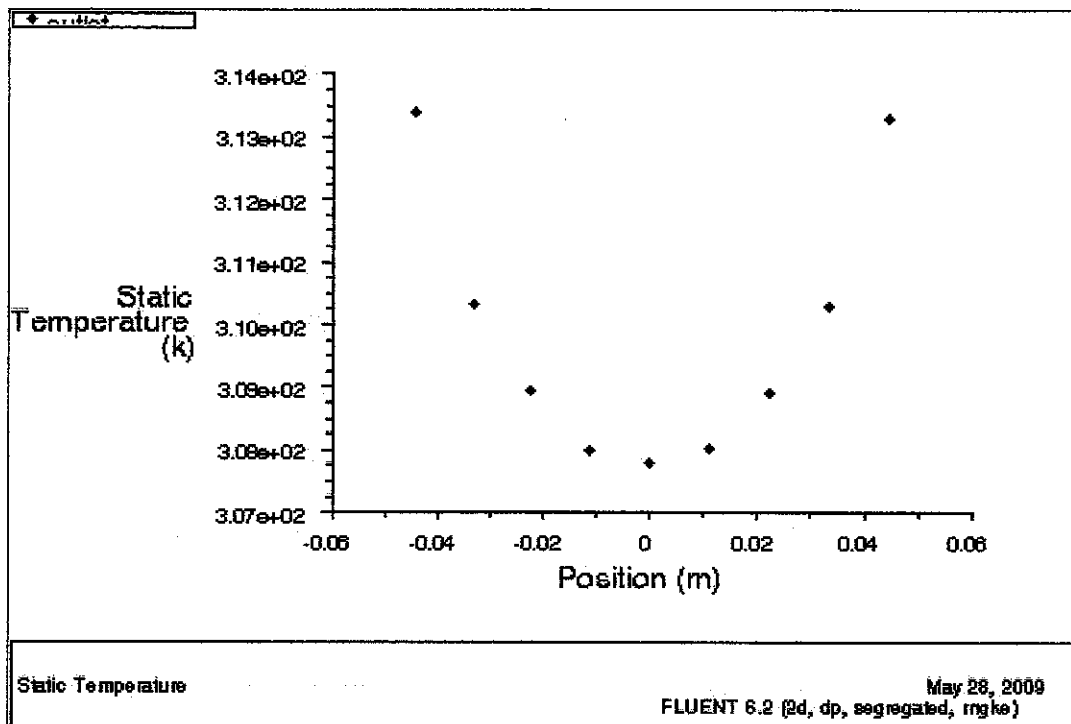


Static Temperature Plot

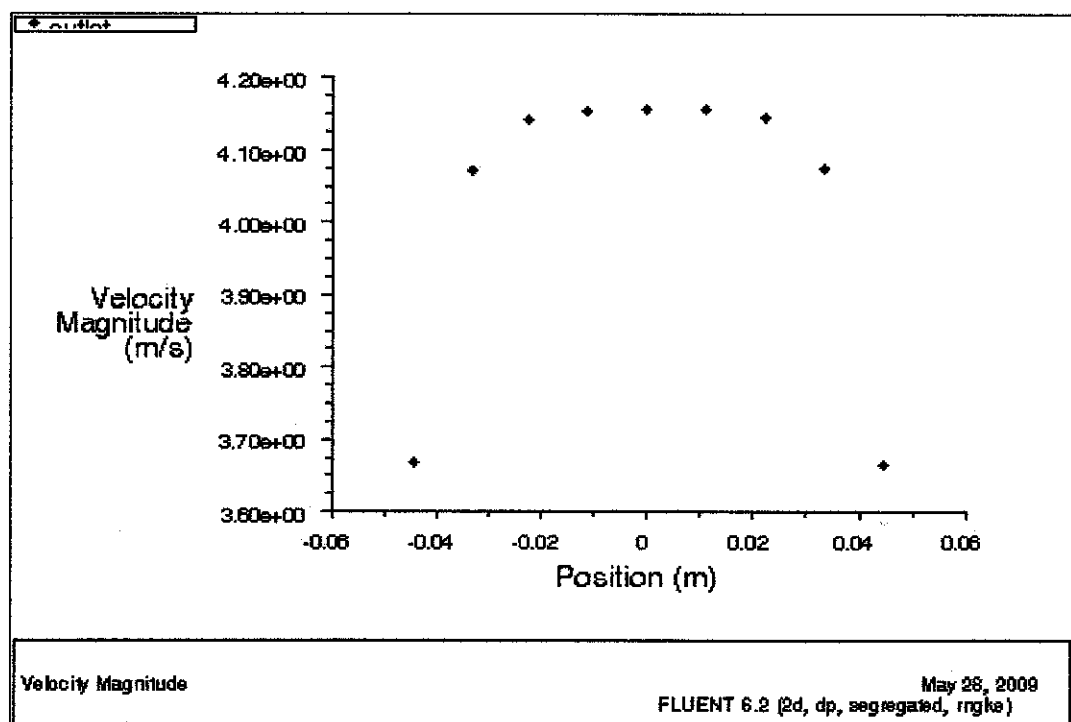


Velocity Magnitude Plot

5.2.9 Case 2, Configuration 3, Option 2b

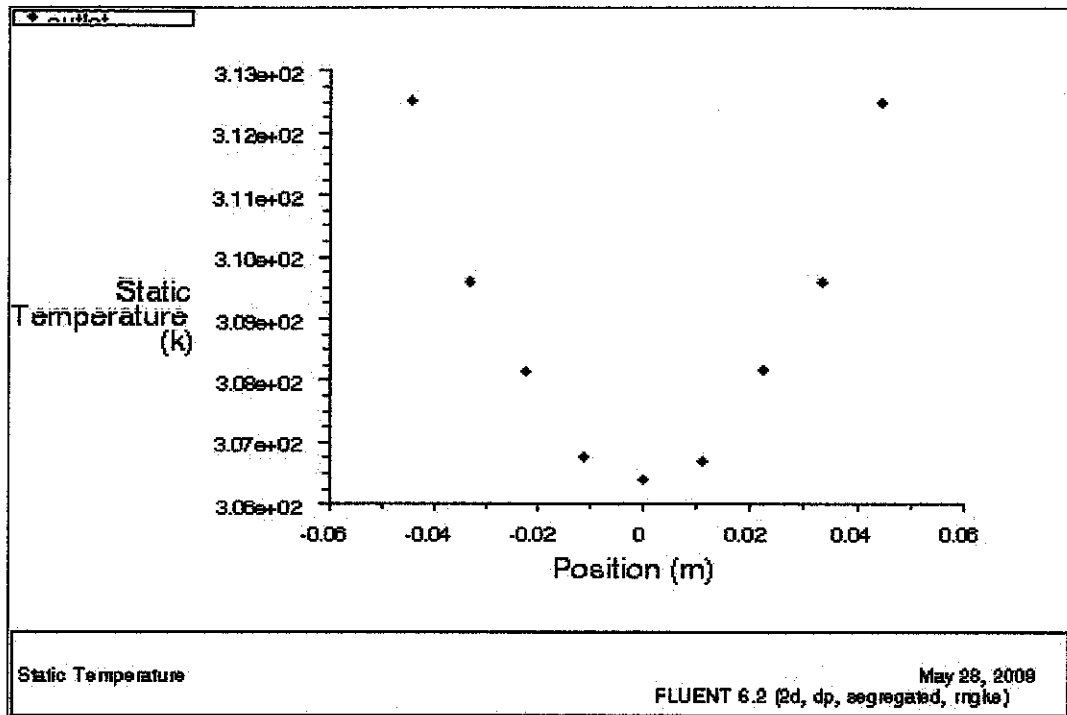


Static Temperature Plot

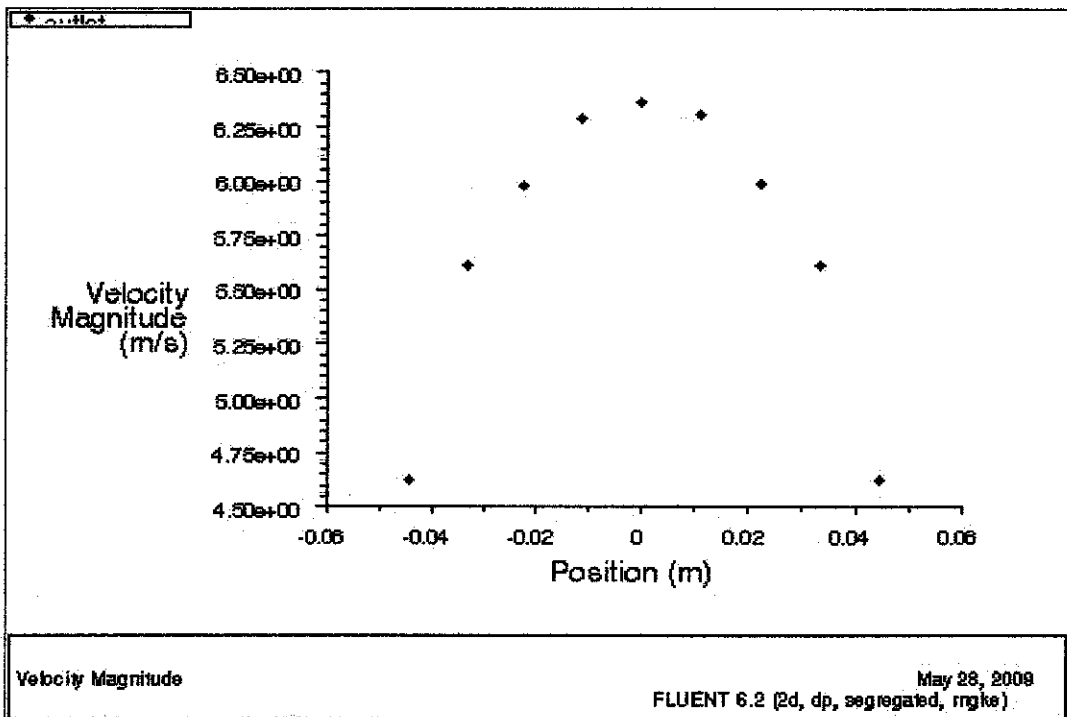


Velocity Magnitude Plot

5.2.10 Case 2, Configuration 3, Option 2c

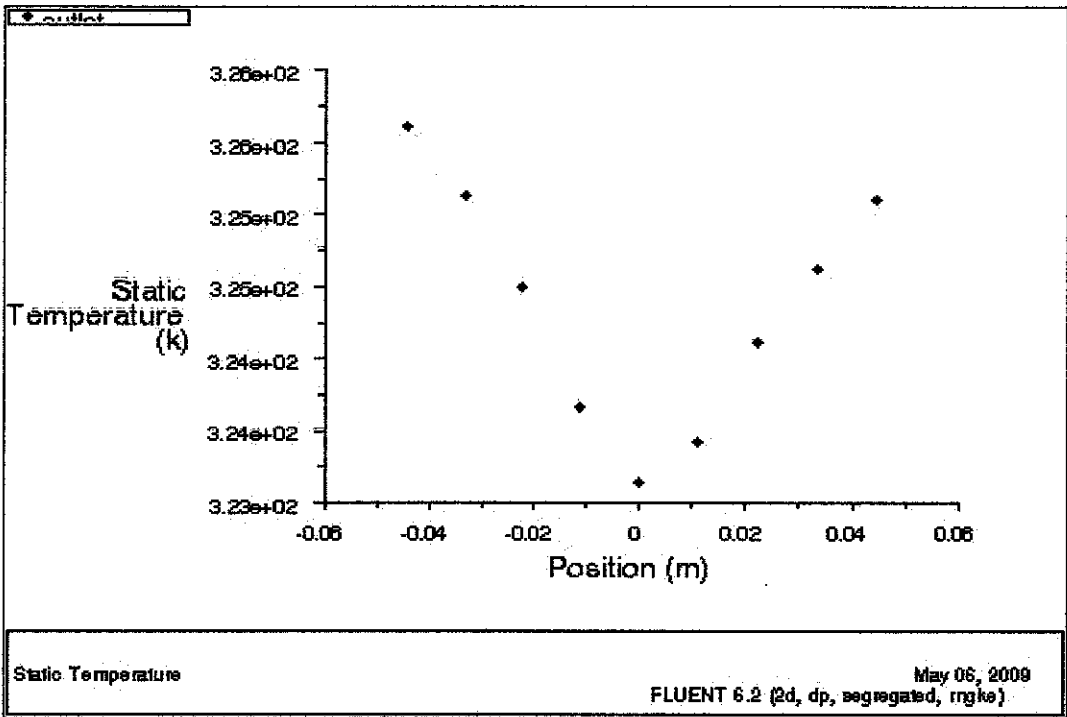


Static Temperature Plot

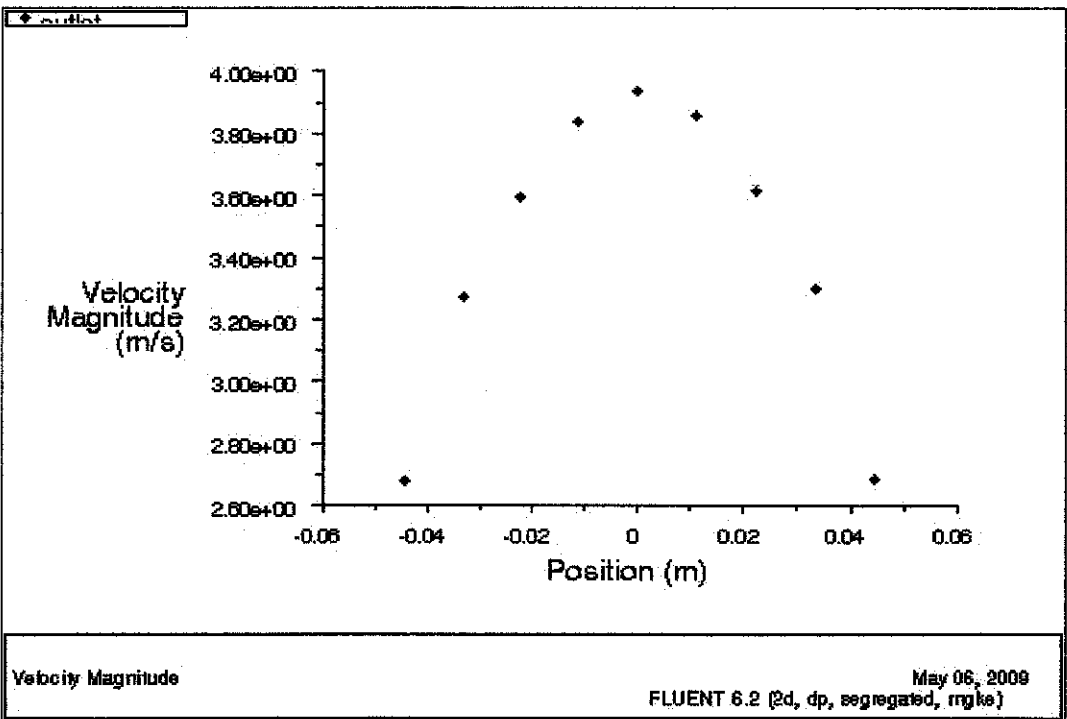


Velocity Magnitude Plot

5.2.11 Case 2, Configuration 4, Option 1a

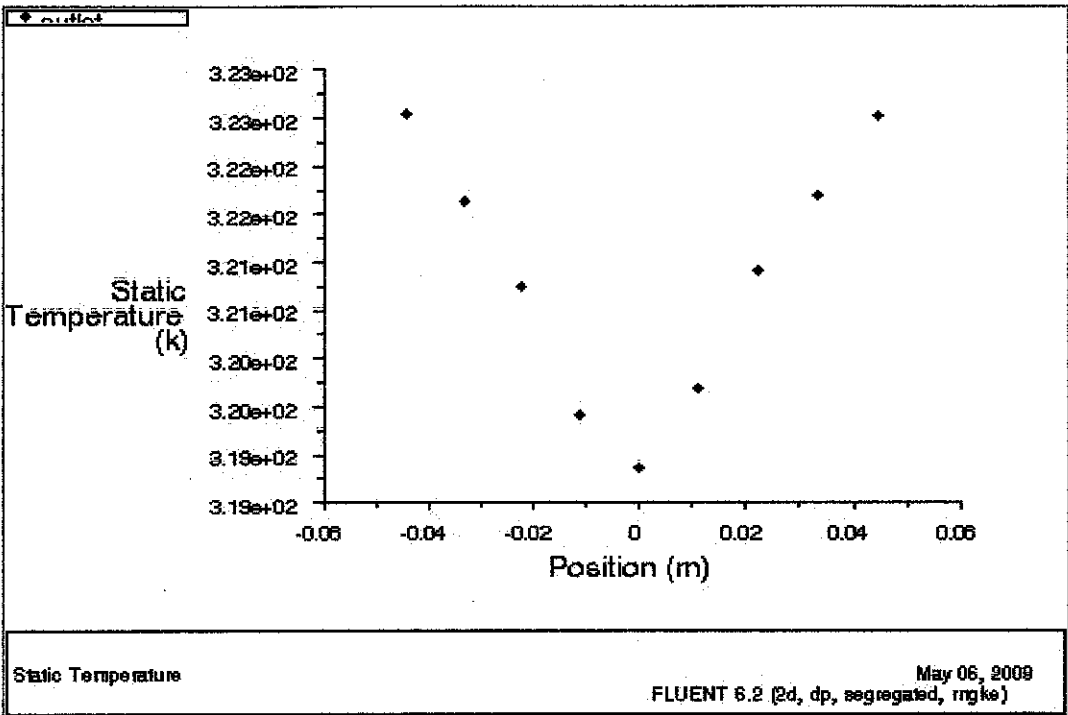


Static Temperature Plot

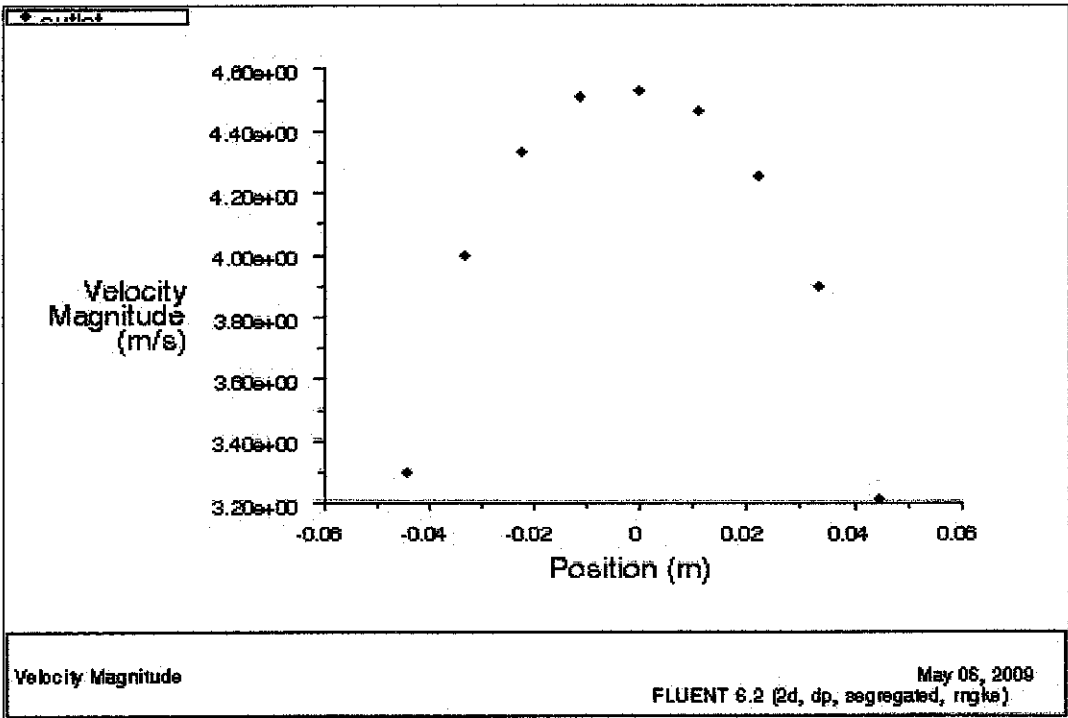


Velocity Magnitude Plot

5.2.12 Case 2, Configuration 4, Option 1b

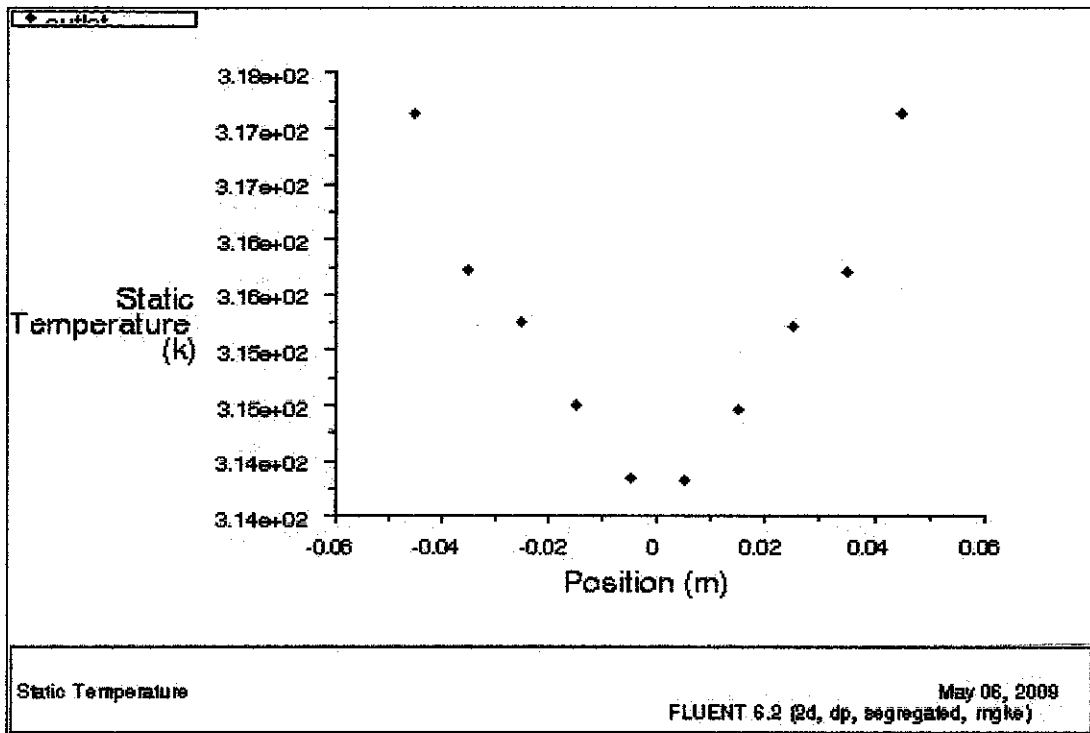


Static Temperature Plot

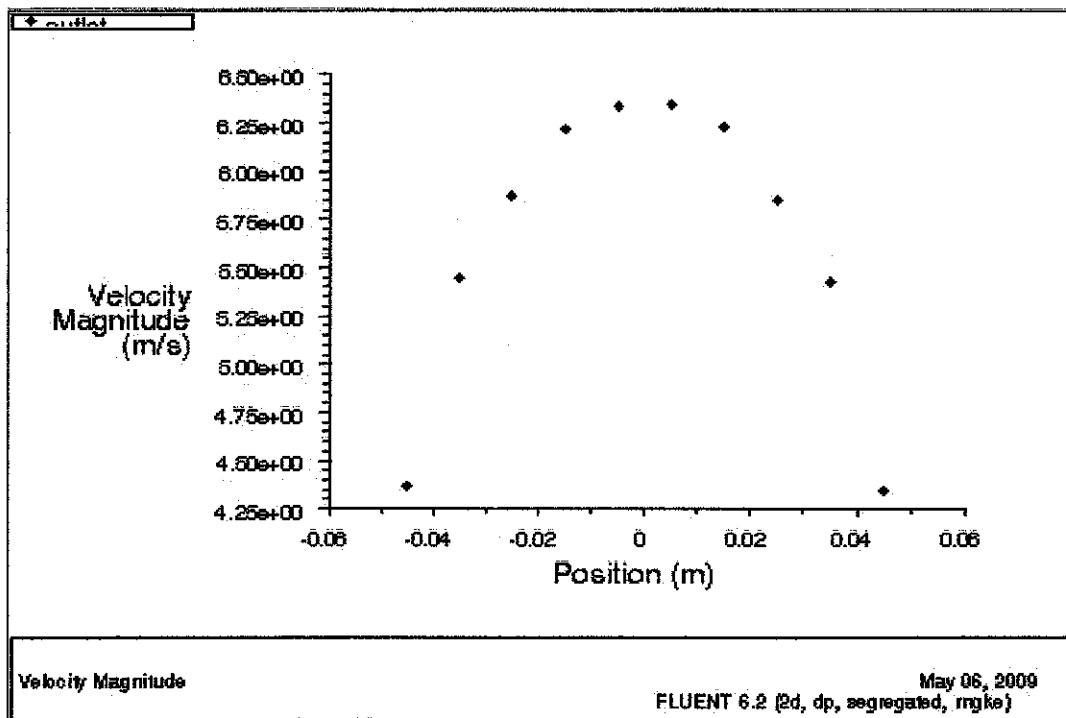


Velocity Magnitude Plot

5.2.13 Case 2, Configuration 4, Option 1c

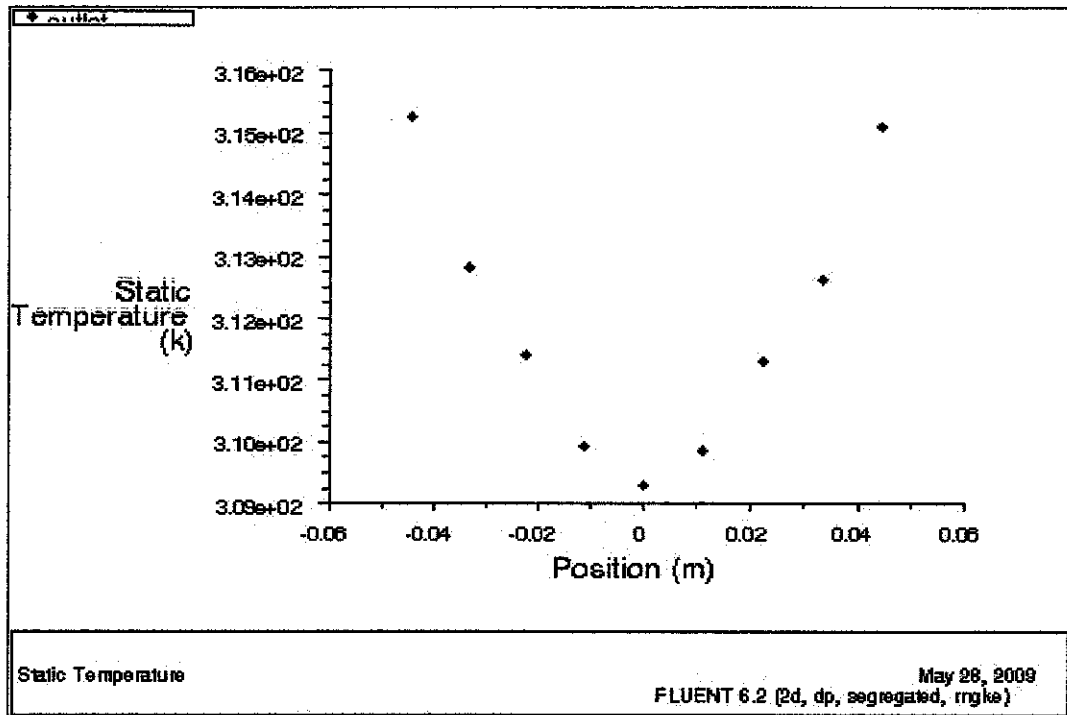


Static Temperature Plot

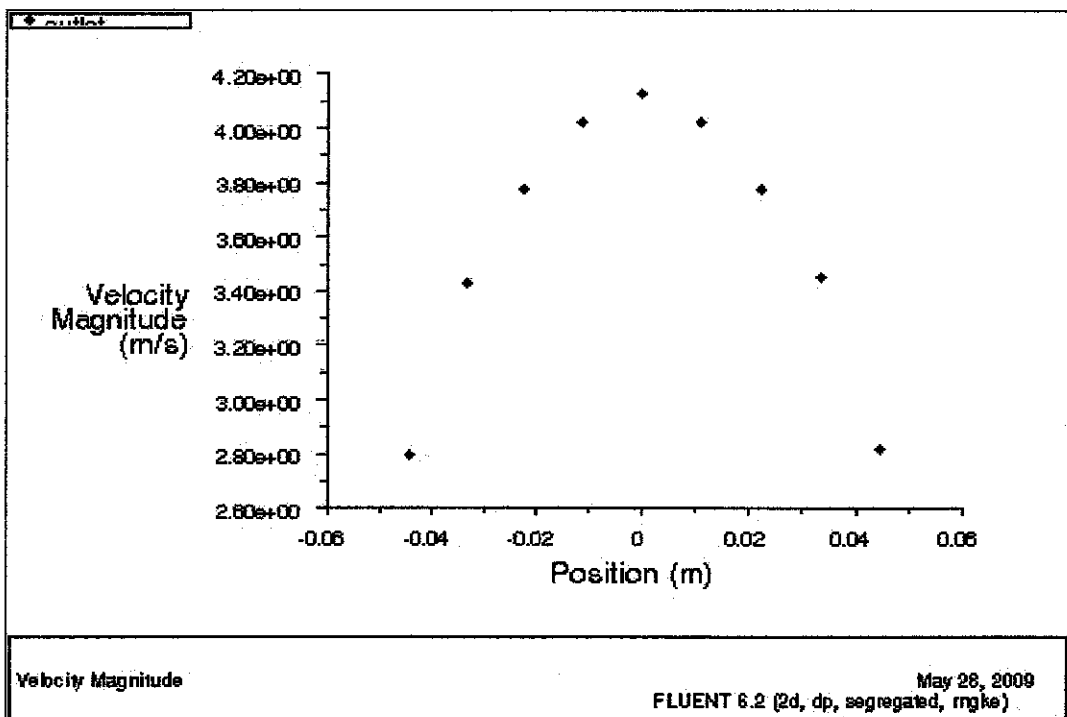


Velocity Magnitude Plot

5.2.14 Case 2, Configuration 4, Option 2a

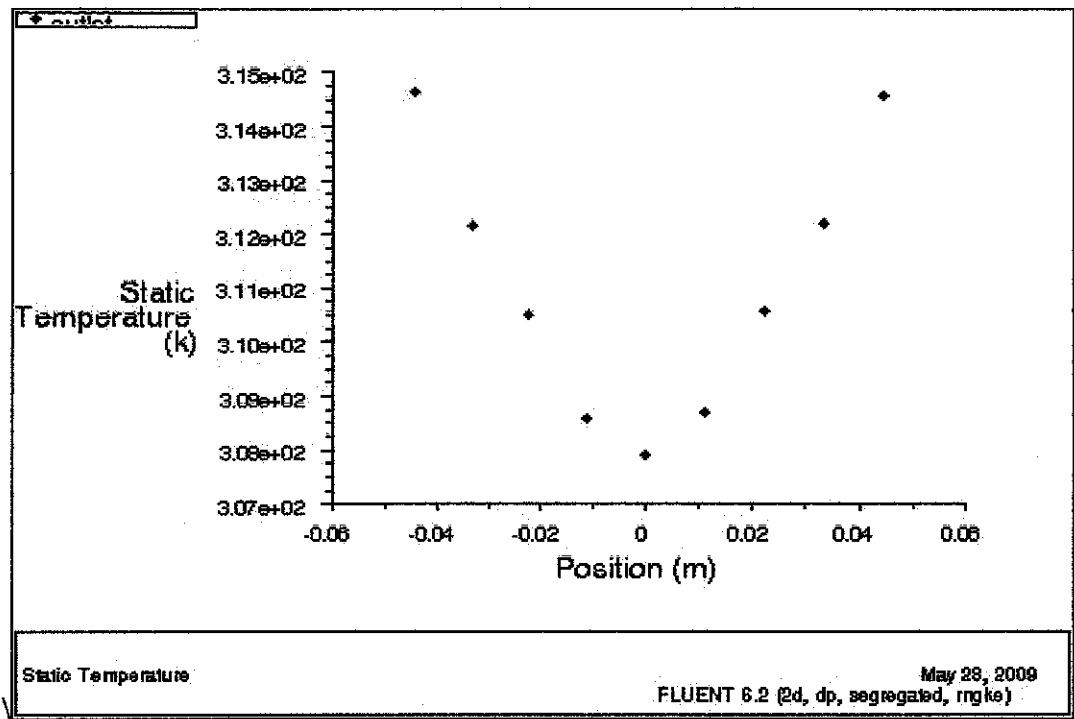


Static Temperature Plot

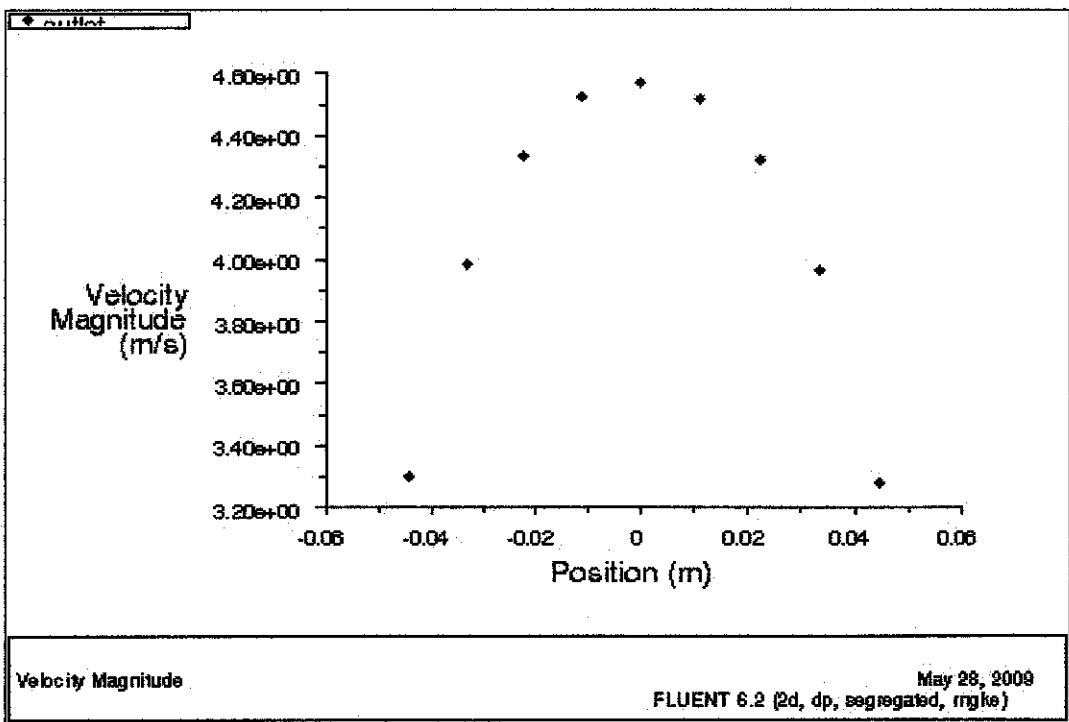


Velocity Magnitude Plot

5.2.15 Case 2, Configuration 4, Option 2b

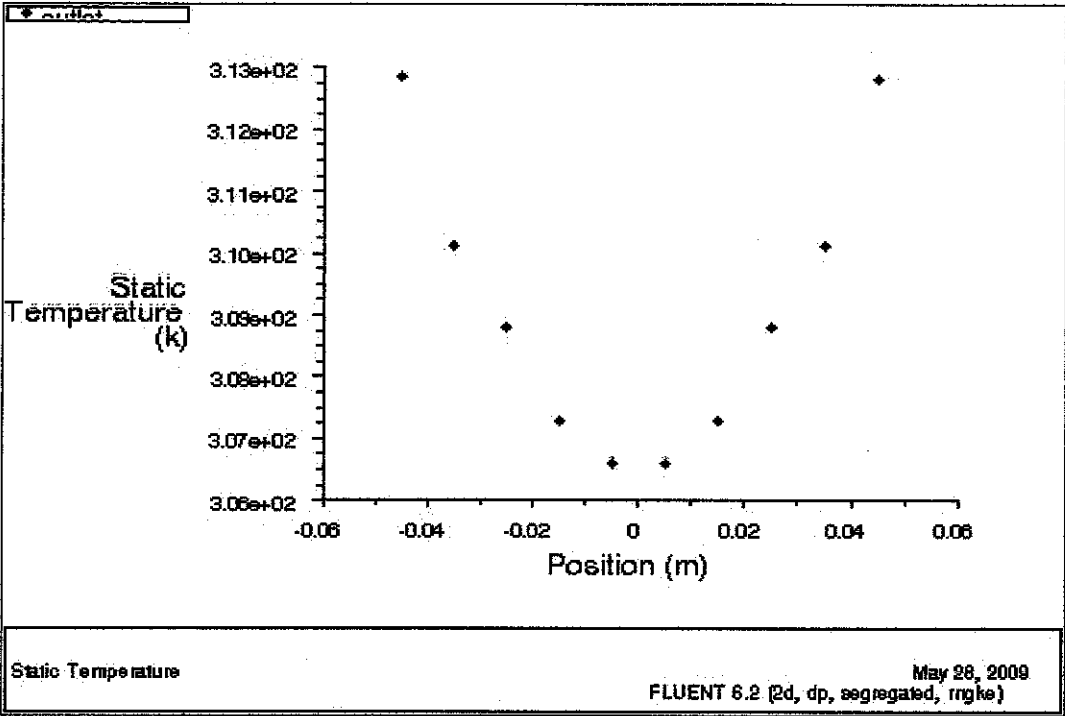


Static Temperature Plot

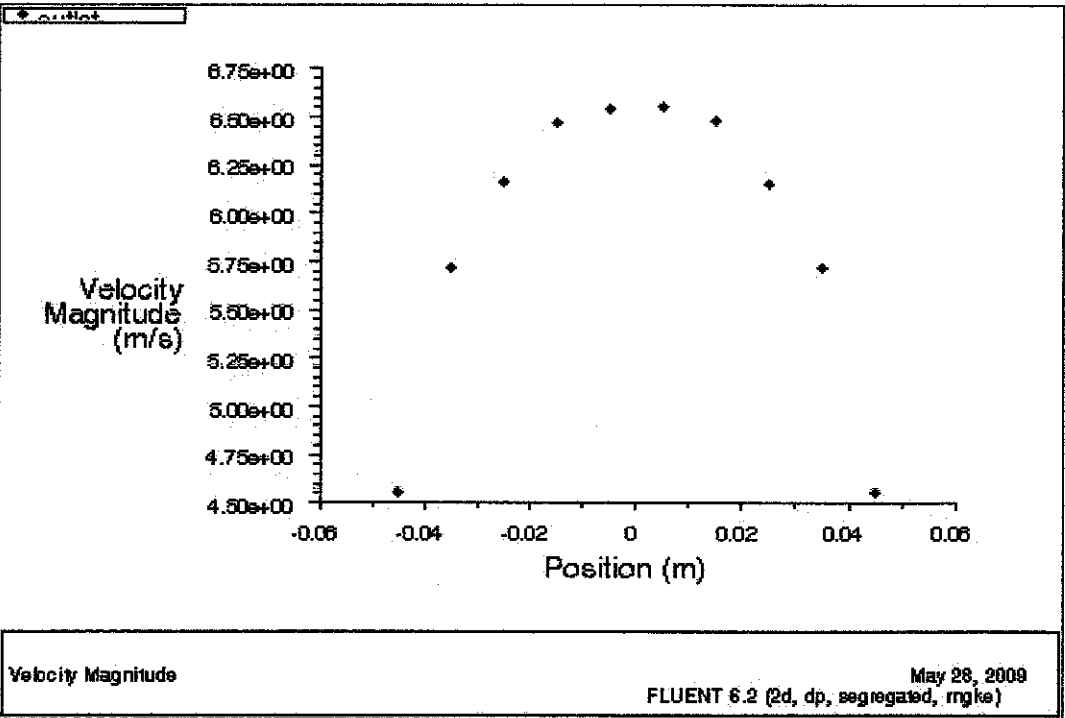


Velocity Magnitude Plot

5.2.16 Case 2, Configuration 4, Option 2c

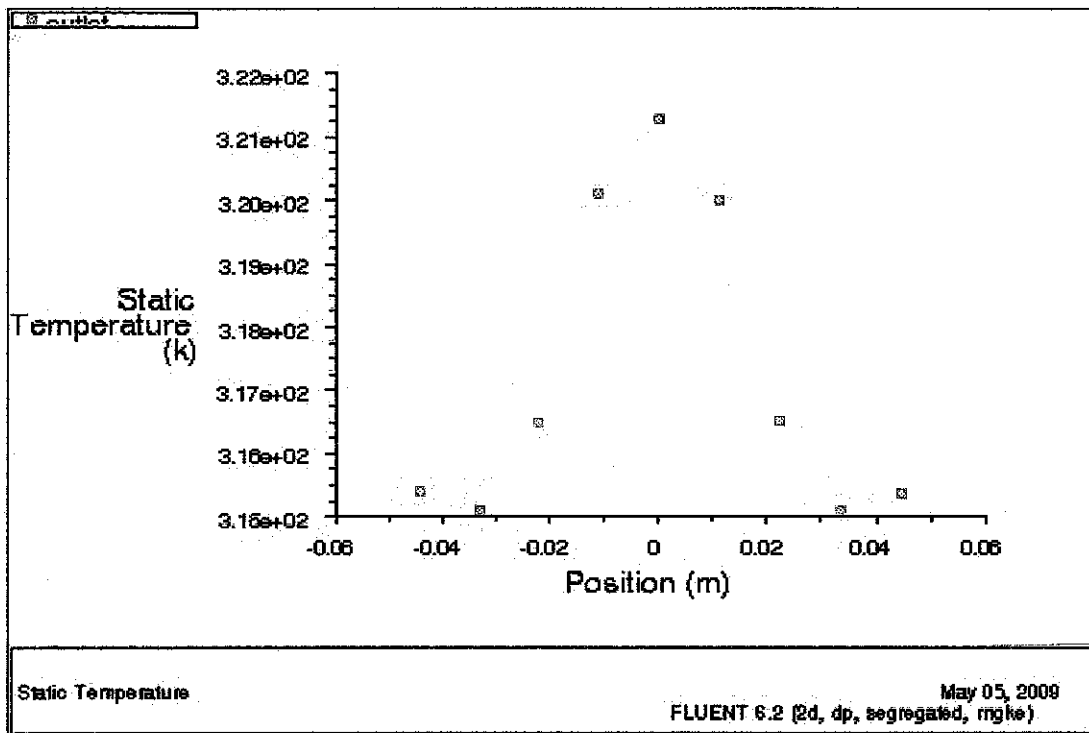


Static Temperature Plot

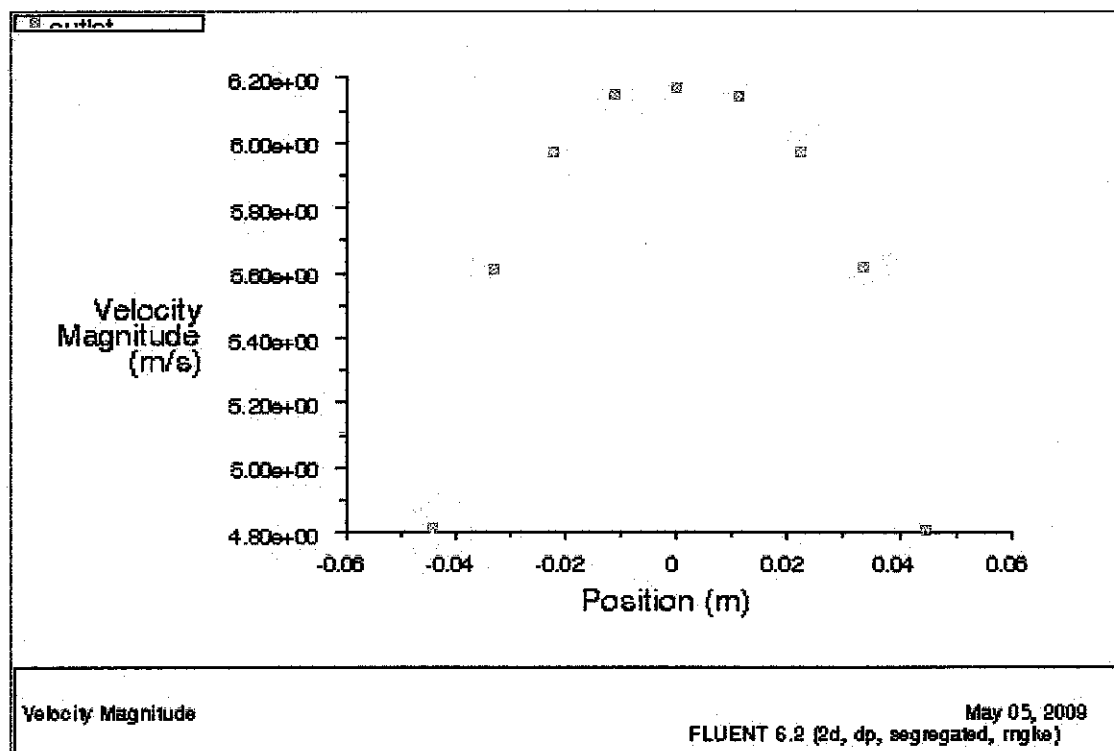


Velocity Magnitude Plot

5.2.17 Case 3, Configuration 5

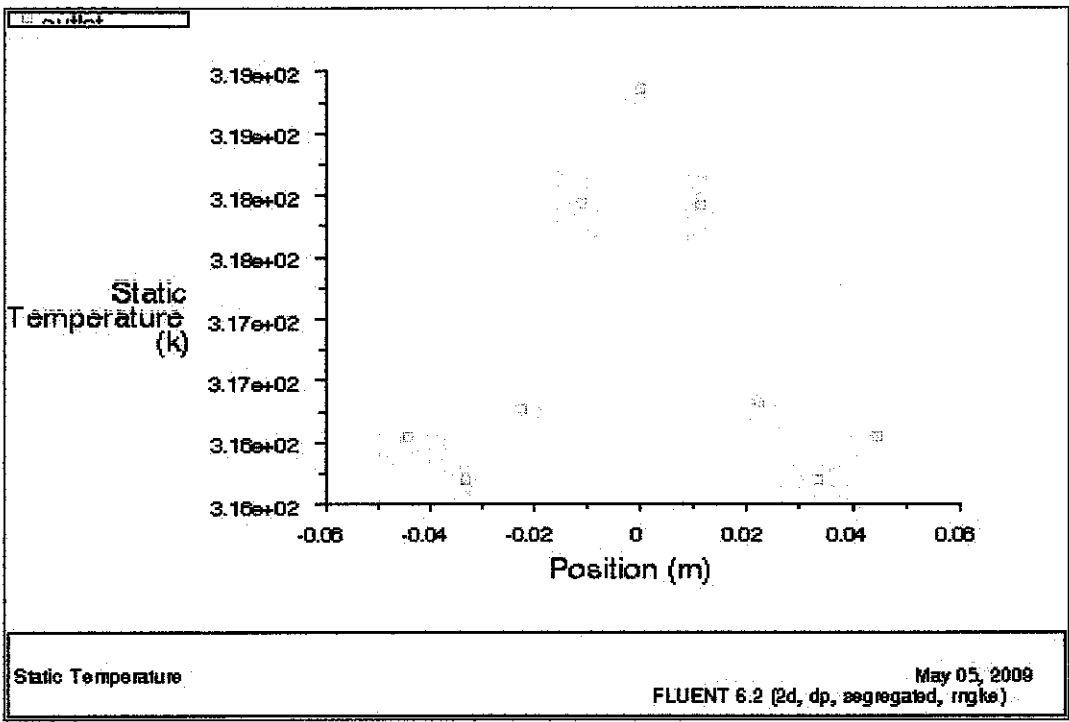


Static Temperature Plot

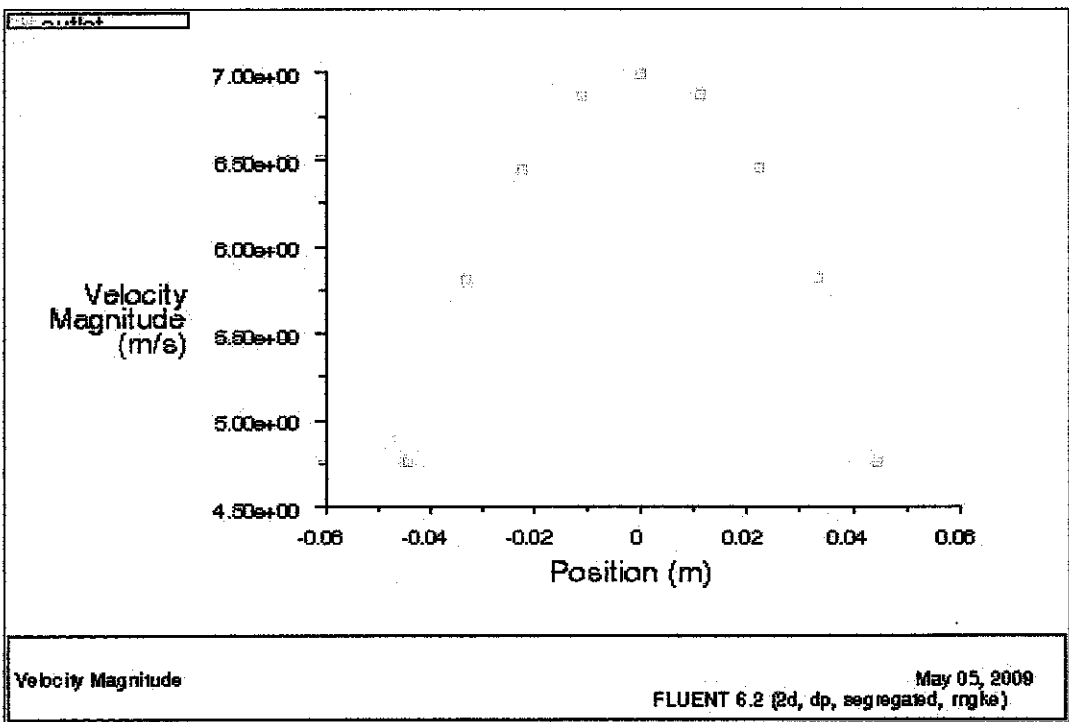


Velocity Magnitude Plot

5.2.18 Case 3, Configuration 6



Static Temperature Plot



Velocity Magnitude Plot

5.3 Velocity, Temperature and Mass Flow Rate

Table 5.1 - FLUENT result on chimney outlet velocity and temperature with mass flow rate from outlet for different configurations and conditions

Details				v (m/s)	T_{out} (K)	T_{in} (K)	ΔT (K)	\dot{m} (kg/s)
Case 1	Configuration 1	Option A		5.204	315.14	304	11.14	1.9047
		Option B		5.381	313.43	304	9.43	1.9694
	Configuration 2	Option A		5.610	314.27	304	10.27	2.0533
		Option B		5.613	313.24	304	9.24	2.0544
Case 2	Configuration 3	Collector Temperature	$D_{in} = 0.050m$	4.046	321.52	304	17.52	1.4809
			$D_{in} = 0.057m$	4.431	315.89	304	11.89	1.6217
			$D_{in} = 0.100m$	6.421	312.55	304	8.55	2.3499
		Convection	$D_{in} = 0.050m$	3.758	309.34	304	5.34	1.3755
			$D_{in} = 0.057m$	4.116	307.55	304	3.55	1.5066
			$D_{in} = 0.100m$	6.361	306.33	304	2.33	2.3279
	Configuration 4	Collector Temperature	$D_{in} = 0.0707m$	3.833	322.86	304	18.86	1.4030
			$D_{in} = 0.0806m$	4.486	318.63	304	14.63	1.6417
			$D_{in} = 0.1414m$	6.250	317.79	304	13.79	2.2874
		Convection	$D_{in} = 0.0707m$	4.111	309.22	304	5.22	1.5047
			$D_{in} = 0.0806m$	4.498	307.90	304	3.90	1.6462
			$D_{in} = 0.1414m$	6.503	306.46	304	2.46	2.3802
Case 3	Configuration 5			6.146	321.20	304	17.20	2.2494
	Configuration 6			6.900	318.71	304	14.71	2.5254

5.4 Discussion

From the result shown above, Configuration 2 and 4 (flat inlet) resulted in higher exit velocity at chimney outlet than Configuration 1 and 3 (trimmed inlet). The reason for configuration 2 yield higher velocity than configuration 1 might be due to larger inlet area. Below shown is the justification for the reason.

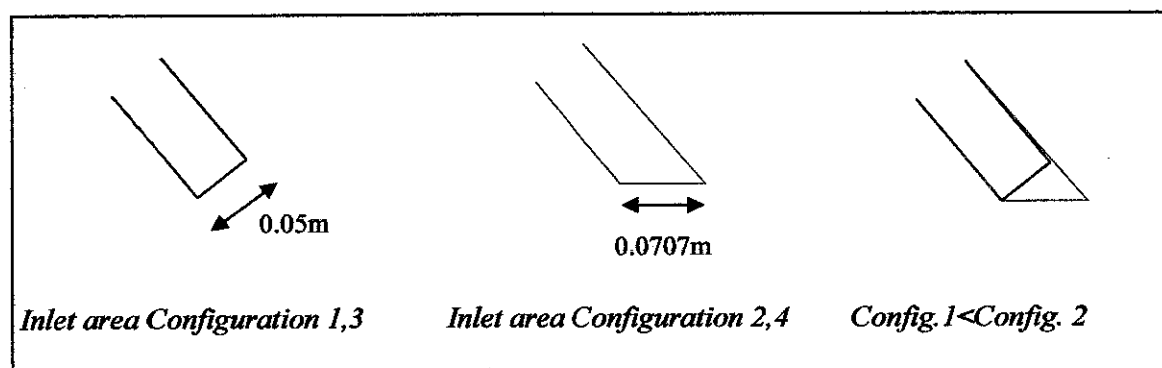


Figure 5.8 - Justification for higher velocity result

The simulations were also run for different types of collector plate shape; corrugated and flat plate area. Shown below is the temperature obtained for two shape of collector.

Table 5.2 - FLUENT result on different types of collector plate

Plate Shape	Flat Plate	Corrugated Plate	Difference
Trimmed inlet (configuration 1)			
Option A	5.204	5.178	0.026
Option B	5.381	5.070	0.311
Flat inlet (configuration 2)			
Option A	5.610	5.450	0.20
Option B	5.613	5.401	0.212

From the table above, it is observed that the velocity differences between flat and corrugated plate are insignificant and it is very small (less than 0.5).

CHAPTER 6

CONCLUSION & RECOMMENDATIONS

6.1 Conclusion

As a conclusion, the objectives of the project are achieved through great supervision by supervisor and with continuous effort of running the simulations in CFD. The requirement of project to run the on-roof solar chimney design with different geometry configurations and with different operating conditions is accomplished. From the CFD simulations result, different chimney inlet areas do affect the outlet velocity. The velocities obtained are near with the experimental value done by previous student. Different collector position and number of surface contact of collector do affect the velocity since variation in heat transfer. Inlet velocity is affected by inlet area, thus, increasing the inlet area give us higher inlet and outlet velocity. Biomass integration with solar chimney is done to observe the effectiveness of using heat from flue gas (recycle the heat). The integration does benefit by increasing the speed of air to reach the chimney outlet with higher velocity.

6.2 Recommendations

Further study on the effect of different inclination angle of solar radiation can be carried out. Additional investigation can be done by varying material for collector and cover. To find the optimum inlet area, investigation using different and bigger inlet diameter than diameter used in this project should be done. It is also recommended to use different dimension of on-roof solar chimney according to

house build in Malaysia of inclination of roof, and integration with other source of biomass or wind.

There are few problems faced during the work progress. The main factor is lack of experts to guide the students on CFD simulations, especially GAMBIT and FLUENT. The recommendation is to provide experts in CFD to facilitate FYP students on how to use and learn it, more than a beginner level. In addition, a medium for the FYP students to clear their doubt also should be provided.

REFERENCES

1. Incropera, De Witt, Bergman and Lavine. 2007, *Introduction to Heat Transfer*, Asia, John Wiley & Sons
2. Hussain H. Al-Kayiem, Quarterly Report 1 STIRF project 09/07.08, Solar–Wind–Biomass Integration for Power Generation Using the External House Roof (stage 1), Malaysia, 2008
3. Hussain H. Al-Kayiem, 2008, Report on Biomass as back-up to the Thermal Solar Systems, Universiti Teknologi PETRONAS
4. Ali Nazarian, Nov.7.2007, Hydrothermal Modeling and Performance Investigation of a Solar Chimney using Savonius Wind Turbine, Final Year Project 1, Universiti Teknologi PETRONAS
5. Nurhusna Bt Yusoff, Apr.2008, Design Calculation and Experimental Analysis of “Over Roof Solar Chimney”, Dissertation for Bachelor of Mechanical Engineering, Universiti Teknologi PETRONAS
6. Thembinkosi Robert Khumalo, May.2008, Analytical and CFD Simulation of on-roof Wind Generator Using Biomass”, Dissertation for Bachelor of Mechanical Engineering, Universiti Teknologi PETRONAS
7. http://www.sciencedirect.com/science?_ob=ArticleURL&_udi=B6V23-48HXMT3-
8. D.J. Harris, N. Helwig, 2006, Solar chimney and building ventilation, *Applied Energy*, Volume 84, Issue 2, February 2007, Pages 135-146

9. Joseph Khedari, Boonlert Boonsri, Jongjit Hirunlabh.1999, "Ventilation impact of a solar chimney on indoor temperature fluctuation and air change in a school building", *Energy and Buildings* 32_2000.89–93

10. Joseph Khedari, Ninnart Rachapradit, Jongjit Hirunlabh. 2001, "Field study of performance of solar chimney with airconditioned building", *Energy* 28 (2003) 1099–1114

11. Tan Boon Thong, Lew Mai Quaan, Ong Kok Seng.2007, "Simulations of Flow in a Solar Roof Collector Driven by Natural Convection", *16th Australasian Fluid Mechanics Conference, Australia*

12. Agung Murti Nugroho, Mohd Hamdan Ahmad, Then Jit Hiung.2006, "Evaluation of parametrics for the development of vertical Solar Chimney ventilation in hot and humid Climate", *2nd International Network for Tropical Architecture conference, Jogjakarta*

13. Jyotirmay Mathur, Sanjay Mathur, Anupma.2005, "Summer-performance of inclined roof solar chimney for natural ventilation" *Energy Building Vol 38, 1156-1163*

14. Agung Murti Nugroho, Mohd Hamdan bin Ahmad. Possibility to use Solar Induced Ventilation Strategies in Tropical Conditions by Computational Fluid Dynamic Simulation.

15. Dr Alan Williams.2005, "Solar Chimney plus Bell Jar"
<http://aesop.rutgers.edu/~horteng/ppt/papers/FloorHeating2.pdf>
 (Date: 15th March 2009, Time: 8.40am)

16. Zoltan Adam, Toshio Yamanaka and Hisashi Kotani." Mathemaical Model and Experimental Study of Airflow in Solar Chimneys"
http://www.globalwarmingsolutions.co.uk/solar_chimney_plus_bell_jar.htm
 (Date: 16th March 2009, Time: 8.15am)

APPENDIX

Properties Table

Air properties

Parameter	Symbol	Value	Unit
Mean Temperature	T_m	328.5	K
Conductivity	k	0.028409	W/m.K
Viscosity	ν	0.000018757	m^2/s
Absorptivity	α	0.000026718	m^2/s
Prandtl Number	Pr	0.70301	

Collector and Cover (Canopy) properties

Items	Details	Unit
Collector material	Aluminum	
Collector thickness	7	mm
▪ Density	2179	kg/m^3
▪ Specific heat	871	J/kg.K
▪ Thermal conductivity	202.4	W/m.K
Canopy material	Perspex	
Canopy thickness	2	mm
▪ Density	1190	kg/m^3
▪ Specific heat	840	J/kg.K
▪ Thermal conductivity	0.9	W/m.K

Hydraulic Diameter, D_h for corrugated and flat plate collector

Plate Shape	Inlet D_h	Outlet D_h
<i>Trimmed inlet (configuration 1)</i>		
Flat Plate	0.09836	0.1935
Corrugated Plate	0.09894	
<i>Flat inlet (configuration 2)</i>		
Flat Plate	0.1368	0.1935
Corrugated Plate	0.1380	

Sample Calculation for Hydraulic Diameter

i) Roof Inlet

For Configuration 1 + Flat Plate

$$A = 3\text{m} \times 0.05\text{m} = 0.15\text{m}^2$$

$$P = 2 (3\text{m} + 0.05\text{m}) = 6.1\text{m}$$

$$D_h = 4A/P = 4(0.15\text{m}^2)/6.1\text{m} = \mathbf{0.09836\text{m}}$$

For Configuration 1 + Corrugated Plate

$$A = (3\text{m}) \times 0.05\text{m} = 0.2356\text{m}^2$$

$$P = 2 (3\text{m} \times \pi/2 + 0.05\text{m}) = 9.5248\text{m}$$

$$D_h = 4A/P = 4(0.2356\text{m}^2)/ 9.5248\text{m} = \mathbf{0.09894\text{m}}$$

ii) Chimney Outlet

$$A = 3\text{m} \times 0.1\text{m} = 0.3\text{m}^2$$

$$P = 2 (3\text{m} + 0.1\text{m}) = 6.2\text{m}$$

$$D_h = 4A/P = 4(0.3\text{m}^2)/6.2\text{m} = \mathbf{0.1935\text{m}}$$

Hydraulic diameter, D_h for each configuration of Case 2

Configuration	Configuration 3			Configuration 4		
$D_{in} \text{ (m)}$	0.050	0.057	0.100	0.0707	0.0806	0.1414
$D_h \text{ (m)}$	0.09836	0.11187	0.1935	0.1368	0.1395	0.2701

Convection Coefficient, \bar{h} Calculation

For second case (Case 2), where two –side collector surface contact is assumed, convection coefficient, \bar{h} have to be determined to run the simulation for heat transfer concern. Thus, calculation shown below is used to determine the \bar{h} value.

Charateristic length, L_c
$$L_c = \sqrt{\frac{A_s}{4\pi}}$$

Where A_s for cuboid shape of height, d with a rectangular footprint of width $a \times b$ is

$$\begin{aligned} A_s &= 2(a \times b) + 2(a \times d) + 2(b \times d) \\ &= 2(3 \times 1.9) + 2(3 \times 0.007) + (1.9 \times 0.007) \\ &= 11.4686 \text{m}^2 \end{aligned}$$

Thus, $L_c = \sqrt{\frac{11.4686}{4\pi}} = 0.9553$

$$Ra_L = \frac{g\beta(T_s - T_\infty)L^3}{\nu\alpha}$$

Values that substituted in Rayleigh equation is calculated as follows;

$$T_m = \frac{(353 + 304)}{2} = 328.5 \text{K}$$

$$\beta = \frac{1}{328.5} = 0.003044 \text{K}^{-1}$$

$$Ra_L = \frac{(g \cos \theta)\beta(T_s - T_\infty)L^3}{\nu\alpha}$$

$$Ra_L = \frac{(9.81 \cos 45^\circ)(0.003044)(353 - 304)(0.9553)^3}{(18.757 \times 10^{-6})(26.718 \times 10^{-6})} = 1.7999 \times 10^9$$

The Nusselt number, Nu for the flow inside the channel is calculated from

$$\overline{Nu}_L = \left\{ 0.825 + \frac{0.387(1.7999 \times 10^9)^{1/6}}{\left[1 + (0.492/0.70301)^{9/16} \right]^{8/27}} \right\}^2 = 147.1735$$

Since,

$$\overline{Nu}_L = \frac{\bar{h}L}{k} \rightarrow \bar{h} = \frac{\overline{Nu}_L k}{L}$$

Thus,

$$\bar{h} = \frac{\overline{Nu}_L k}{L} = \frac{(147.1735)(28.409 \times 10^{-3})}{0.9553} = 4.3767$$

Later, for each configurations, mass flow rate at chimney outlet is calculated as

$$\dot{m} = \rho A V$$

Where

$$\rho_{\text{air}} = 1.22 \text{ kg/m}^3$$

$$A = 3 \times 0.1 = 0.3 \text{ m}^2$$

V = outlet velocity

Inlet pressure estimation

$$P = \rho gh$$

where

h = difference of height of outlet point to inlet point

$$P_m = \rho_{\text{air}} gh = (1.22 \text{ kg/m}^3) \cdot (9.81 \text{ m/s}^2) \cdot [1 - (-1.4496)] = 29.3173 \text{ Pa} \approx 29 \text{ Pa}$$